

# On the tidal evolution of Hot Jupiters on inclined orbits

Adrian J. Barker\* and Gordon I. Ogilvie

*Department of Applied Mathematics and Theoretical Physics, University of Cambridge, Centre for Mathematical Sciences, Wilberforce Road, Cambridge CB3 0WA, UK*

Accepted 2009 February 25. Received 2009 February 24; in original form 2009 January 16

## ABSTRACT

Tidal friction is thought to be important in determining the long-term spin-orbit evolution of short-period extrasolar planetary systems. Using a simple model of the orbit-averaged effects of tidal friction (Eggleton et al. 1998), we study the evolution of close-in planets on inclined orbits, due to tides. We analyse the effects of the inclusion of stellar magnetic braking by performing a phase-plane analysis of a simplified system of equations, including the braking torque. The inclusion of magnetic braking is found to be important, and its neglect can result in a very different system history. We then present the results of numerical integrations of the tidal evolution equations, where we find that it is essential to consider coupled evolution of the orbital and rotational elements, including dissipation in both the star and planet, to accurately model the evolution.

The main result of our integrations is that for typical Hot Jupiters, tidal friction aligns the stellar spin with the orbit on a similar time as it causes the orbit to decay. This tells us that if a planet is observed to be aligned, then it probably formed coplanar. This reinforces the importance of Rossiter-McLaughlin effect observations in determining the degree of spin-orbit alignment in transiting systems.

We apply these results to the only observed system with a spin-orbit misalignment, XO-3, and constrain the efficiency of tidal dissipation (i.e. the modified tidal quality factors  $Q'$ ) in both the star and the planet in this system. Using a model in which inertial waves are excited by tidal forcing in the outer convective envelope and dissipated by turbulent viscosity, we calculate  $Q'$  for a range of F-star models, and find it to vary considerably within this class of stars. This means that using a single  $Q'$ , and assuming that it applies to all stars, is probably incorrect. In addition, we propose an explanation for the survival of two of the planets on the tightest orbits, WASP-12 b and OGLE-TR-56 b, in terms of weak dissipation in the star, as a result of their internal structures and slow rotation periods.

**Key words:** planetary systems – stars: rotation – celestial mechanics – binaries: close – stars: XO-3 – planetary systems: XO-3

## 1 INTRODUCTION

Since the discovery of the first extrasolar planet around a solar-type star (Mayor & Queloz 1995), observers have now detected more than 300 planets<sup>1</sup> around stars outside the solar system. Many of these planets have roughly Jovian masses and orbit their host stars in orbits with semi-major axes less than 0.1 AU, the so-called “Hot Jupiters” (HJs). In both of the giant planet formation scenarios (see Papaloizou & Terquem 2006 for a comprehensive review), core accretion and gravitational instability, it is difficult to produce HJs in situ. Close-in planets are likely to form in colder regions of

the protoplanetary disc, much further out ( $a \sim$  several AU), before a migratory process brings the planet in towards the star and to its present location (Lin et al. 1996).

The formation of systems of giant planets can be thought of as occurring in two oversimplified stages (Jurić & Tremaine 2008). During stage 1 the cores of the giant planets are formed, they accrete gas and undergo migration, driven by the dynamical interaction between the planets and the gaseous protoplanetary disc (see Papaloizou et al. 2007 for a recent review). This stage lasts a few Myr until the gas dissipates, by which time a population of gas giants may exist. If these form sufficiently closely packed then stage 2 follows (some evidence in favour of such packing in multiple-planet systems is given by Barnes & Greenberg 2007). This stage lasts from when the disc has dissipated until the present,

\* E-mail: [ajb268@cam.ac.uk](mailto:ajb268@cam.ac.uk)

<sup>1</sup> see <http://exoplanet.eu/> for the latest updates

and primarily involves gravitational interactions and collisions between the planets. Recent studies of stage 2 (Juric & Tremaine 2008; Chatterjee et al. 2008; Ford & Rasio 2008) have shown that this is a chaotic era, in which planet–planet scatterings force the ejection of all but a few ( $\sim 2 - 3$ ) planets from the system, in a period of large-scale dynamical instability lasting  $\lesssim 10^8$  yr. This mechanism can excite the eccentricities of the planets to levels required to explain observations.

Planet–planet scatterings tend also to excite the inclinations of the planets with respect to the initial symmetry plane of the system (Juric & Tremaine 2008), though this has been found to be less efficient than the excitation of eccentricity. This potentially leads to observable consequences via the Rossiter–McLaughlin (RM) effect (Rossiter 1924; McLaughlin 1924; Winn et al. 2005).

The RM effect is a spectral distortion of the radial velocity data that results from the planet occulting a spot on the rotating surface of the star as it transits the stellar disc. High-precision radial velocity data during a transit allow a determination of the angle ( $\lambda$ ) between the sky-projected angular momentum vectors of the planetary orbit ( $\mathbf{h}$ ) and stellar spin ( $\mathbf{\Omega}$ ), through the RM effect. This measured value  $\lambda$  is not necessarily the same as the inclination (or stellar obliquity)  $i$ , which is the angle between the equatorial plane of the star and orbital plane of the planet (defined by  $\cos i = \hat{\mathbf{\Omega}} \cdot \hat{\mathbf{h}}$ ), since  $\lambda$  is just a sky-projection of this angle. Nevertheless,  $\lambda$  gives a lower bound on the angle between these two vectors, and they are related by  $\cos i = \cos I_* \cos I_p + \sin I_* \sin I_p \cos \lambda$ , where  $I_p$  and  $I_*$  are the angles of inclination of the planetary orbital plane and stellar equatorial plane, to the plane of the sky. For a transit, the orbit must be close to edge-on, so  $I_p \sim 90^\circ$ , giving  $\cos i \simeq \sin I_* \cos \lambda$ .

The RM effect has now been used to measure the degree of spin–orbit alignment in 11 systems (Winn 2008), though this number is expected to grow rapidly over the next few years. These systems are currently all consistent with  $\lambda$  being zero, with the exception of XO-3 b (Hébrard et al. 2008), which is discussed in §8.1 below.

It is possible for HJs orbiting a host star which has a distant and inclined stellar companion, or massive inclined outer planetary companion, to undergo another type of migration. This is Kozai migration (Wu & Murray 2003). The presence of such an outer companion to an exoplanet host star could cause Kozai oscillations, which produce periods of extreme eccentricity in the planetary orbit, if various conditions are satisfied (e.g. see section 1.2 of Fabrycky & Tremaine 2007). The subsequent tidal dissipation that occurs during the periods of small pericentre distance leads to gradual inward migration of the planet. It has even been proposed that a combination of planet–planet scattering, tidal circularisation and the Kozai mechanism using outer planets, can produce HJs around single stars (Nagasawa et al. 2008). HJs produced from these processes generally have their orbital angular momentum vector misaligned with respect to the stellar spin axis by large angles – occasionally larger than  $90^\circ$  (Fabrycky & Tremaine 2007; Nagasawa et al. 2008).

Misaligned orbits are not predicted from stage 1 alone, so if  $\lambda$  is measured to be appreciably nonzero in enough systems, then it could be seen as evidence for planet–planet

scattering or Kozai migration. This is because gas–disc migration does not seem able to excite orbital inclination (Lubow & Ogilvie 2001; Cresswell et al. 2007). Alternatively, if observed planets are all found with  $\lambda$  consistent with zero, this could rule out planet–planet scattering or Kozai migration as being of any importance.

One important consideration is that at such close proximity to their parent stars, strong tidal interactions between the star and planet are expected to cause significant long-term spin–orbit evolution, including changes to the value of  $\lambda$  (actually the true spin–orbit misalignment angle  $i$ ) over time. If tides can change  $\lambda$  since the time of formation, then we may have difficulty in distinguishing migration caused by planet–planet scattering and Kozai oscillations, from gas–disc migration. The tidal evolution of such inclined orbits must therefore be considered an important goal in planetary evolution studies. In this paper we approach the problem of studying the effects of tidal friction on such inclined orbits.

## 2 PREVIOUS WORK ON TIDAL EVOLUTION RELEVANT TO CLOSE-IN PLANETS

There has been much recent interest into the subject of tidal evolution, and our work can be considered to follow on from some of the more recent developments in the field. Witte & Savonije (2002) studied the effects of stellar spin–down on tidal evolution. They developed a sophisticated model including the effects of stellar evolution, resonance locking and magnetic braking. They studied dynamical tides in solar-type stars, and found that the spin–down due to magnetic braking causes resonance locking to become more intense, which leads to faster orbital decay of a planet.

Dobbs-Dixon et al. (2004) also studied the effects of stellar spin–down, though they considered equilibrium tides, and we adopt the same model of tidal friction. They studied tidal eccentricity evolution, and proposed an explanation for the coexistence of both circular and eccentric orbits for the planets in the period range 7–21 days, the so-called borderline planets, as the result of the variation in spin–down rates of young stars. Planets with orbital periods less than 6 days are sufficiently close to their host stars for tidal dissipation in the planet to be mostly able to account for their negligible eccentricities. Those with periods longer than 21 days are negligibly affected by tides and have been observed with a range of eccentricities, so the borderline planets are referred to as such since they lie in the crossover between these two regimes. Both of these works highlight the importance of studying the effects of stellar spin–down on tidal evolution.

Recently Pont (2008) discussed empirical evidence for tidal spin–up of exoplanet host stars, and found indications of such a process occurring in the present sample of transiting planets. He also proposed that the mass–period relation of close-in planets could be accounted for by tidal transfer of angular momentum from the orbit to the spin of the star. We must note, however, that angular momentum losses from the system due to magnetic braking are likely to change this picture considerably. In particular, the attainment of a spin–orbit synchronous state becomes questionable when angular momentum is being removed from the system – this is dis-

cussed in §5 below. We note that his conclusions also depend on assumptions regarding the stellar  $Q'$  – see §3.1.

Jackson et al. (2008a) found that simple timescale considerations of circularisation may not accurately represent the true evolution from considering coupled evolution of the eccentricity and semi-major axis. In addition, they found that it is inaccurate to neglect the combined effects of the stellar and planetary tides in computing the evolution.

Here we aim to study the accuracy of the simple timescale estimates for tidal evolution, when coupled evolution of the orbital and rotational elements is considered, in a more general model of the long-term effects of tidal friction than Jackson et al. (2008a) consider. We include stellar spin-down, and study its effects in a simplified system. In particular, we investigate the tidal evolution of inclination, since this has not been done in previous studies.

### 3 MODEL OF TIDAL FRICTION ADOPTED

#### 3.1 General introduction to tidal friction

The tidal interaction between two orbiting bodies acts to continually change the orbital and rotational system parameters, and continually dissipates energy. Ultimately – in the absence of angular momentum loss from the system – either an equilibrium state is asymptotically approached, or the two bodies spiral towards each other at an accelerating rate, and eventually collide. The equilibrium state is characterised by coplanarity (the equatorial planes of the bodies coincide with the orbital plane), circularity and corotation (rotational frequencies of each body match the orbital frequency) (Hut 1980).

The efficiency of tidal dissipation in a body is often parametrised by a dimensionless quality factor  $Q$ , which reflects the fact the body undergoes a forced oscillation and dissipates a small fraction of the associated energy during each oscillation period. This is analogous to the quality factor in a forced, damped harmonic oscillator (Murray & Dermott 1999), and is defined by

$$Q = 2\pi E_0 \left( \oint -\dot{E} dt \right)^{-1},$$

where  $E_0$  is the maximum energy stored in an oscillation and the integral represents the energy dissipated over one cycle. This is related to the time lag  $\tau$  in the response of the body to tidal forcing of frequency  $\hat{\omega}$  by  $Q^{-1} = \hat{\omega}\tau$ , when  $Q \gg 1$ . We find it convenient to define  $Q' = \frac{3Q}{2k}$ , where  $k$  is the second-order potential Love number of the body, since this combination always appears together in the evolutionary equations.  $Q'$  reduces to  $Q$  for a homogeneous fluid body, where  $k = \frac{3}{2}$ .

The problem of determining the efficiency of tidal dissipation, and therefore quantifying the evolution of the system, amounts to calculating  $Q'$  factors for each body.  $Q'$  is a function of the tidal frequency (and possibly the amplitude of the tidal disturbance), being the result of complex dissipative processes in each body (Zahn 2008). For rotating fluid bodies, such as giant planets and stars, calculations of the excitation and dissipation of internal waves have indicated that  $Q'$  varies in a complicated way with the tidal frequency (see Savonije et al. 1995; Savonije & Papaloizou

1997; Papaloizou & Savonije 1997; Ogilvie & Lin 2004, hereafter OL04; Ogilvie & Lin 2007, hereafter OL07). These calculations rely on a variety of approximations and involve uncertainties, particularly regarding the interaction of the waves with convection.

Typically assumed values of  $Q' \sim 10^6$  for stars are roughly consistent with observational data regarding the circularisation periods of binary stars (OL07). In addition, the magnitude of  $Q$  for HJs is often assumed to be similar to that for Jupiter, which has been inferred to be in the range  $6 \times 10^4 - 2 \times 10^6$  (Yoder & Peale 1981). This estimate is based on a model of the tidal origin of the Laplace resonance among the Galilean satellites; however, it has been argued that even if the origin of the resonance is primordial, the average  $Q$  cannot be far from these bounds (Peale & Lee 2002) – giving  $Q' \sim 10^6$  (since  $k \simeq 0.38$  for Jupiter). This estimate also appears consistent with the work of Jackson et al. (2008a), who found that one can reproduce the outer planet ( $a > 0.2$  AU) eccentricity distribution from integrating the tidal evolution equations backwards in time for the observed close-in planets ( $a < 0.2$  AU) quite well if  $Q \sim 10^{5.5}$  for stars and  $Q \sim 10^{6.5}$  for HJs. However, this stellar  $Q'$  is difficult to reconcile with the existence of the planets on the tightest orbits, such as WASP-12 b (Hebb et al. 2008) and OGLE-TR-56 b (Sasselov 2003), since it would imply that the inspiral time for these planets would be much less than the age of the system. That several planets have been found with similarly short periods makes this seem unlikely on probabilistic grounds. Additionally, Jackson et al. (2008a) assume that  $Q'$  is the same for all exoplanet host stars; this may be an oversimplification, as is discussed in §8.2 below.

It would seem more plausible that the relevant stellar  $Q'$  is in fact higher than this, and this is supported by the theoretical work of OL07. They also propose that the efficiency of tidal dissipation in solar-type stars may be different when the orbiting companion is a  $\sim M_\odot$  star in a close binary, than when its orbiting companion is a close-in gas giant planet. This could be a result of differences in the tidal and spin frequencies in the two situations, which may allow the excitation of inertial waves in the convective envelope of the star in the former case but usually not in the latter. It could also be a result of the excitation of internal inertia-gravity modes at the boundary between the convective and radiative zones, and their resulting dissipation in the radiative core of solar-type stars. If these waves are of small amplitude, then they are unlikely to achieve sufficient nonlinearity to prevent coherent reflection from the centre of the star, hence they form global modes, and only weakly contribute to the dissipation (Goodman & Dickson 1998). If these waves achieve sufficient nonlinearity, then they could overturn the local entropy stratification. This may result in wave breaking, which could dissipate energy in the wave, or in incoherent reflection of the waves from the centre of the star, preventing the formation of global modes, and enhancing the dissipation. Simple estimates of when these waves become nonlinear indicate that the waves excited by HJs marginally achieve sufficient nonlinearity to disrupt the reflection of the waves. This is in contrast to the close binary circularisation problem, in which these waves are likely always to achieve sufficient nonlinearity. This may result in much higher  $Q'$  values relevant to the survival of the very

close-in planets, potentially explaining the discrepancy between the circularisation of binary stars and the survival of the very close-in planets.

### 3.2 Model adopted – see Appendix A for details

In light of the uncertainties involved in calculating  $Q'$ , and the difficulty of calculating the evolution when  $Q'$  is a complicated function of  $\hat{\omega}$ , we adopt a simplified model, based on a frequency-independent lag time – though see discussion in Appendix A. We adopt the model of Eggleton et al. (1998), which is based on the equilibrium tide model of Hut (1981). In this formulation, we calculate the evolution of the specific angular momentum of the planetary orbit

$$\mathbf{h} = \mathbf{r} \times \dot{\mathbf{r}} = na^2 \sqrt{1 - e^2} \hat{\mathbf{h}},$$

together with its eccentricity vector  $\mathbf{e}$ , and the stellar and planetary spin vectors  $\boldsymbol{\Omega}_1$  and  $\boldsymbol{\Omega}_2$ . The eccentricity vector has the magnitude of the eccentricity, and points in the direction of periastron, and is defined by

$$\mathbf{e} = \frac{\dot{\mathbf{r}} \times \mathbf{h}}{Gm_{12}} - \hat{\mathbf{r}},$$

where  $m_{12} = m_1 + m_2$  is the sum of the stellar and planetary masses.

Both  $\mathbf{h}$  and  $\mathbf{e}$  are conserved for an unperturbed Keplerian orbit; therefore under weak external perturbations their components vary slowly compared with the orbital period. This allows averaging of the effects of the tidal perturbation over a Keplerian orbit, resulting in a set of secular evolution equations for the rotational and orbital elements.

This formulation is beneficial because it can treat arbitrary orbital eccentricities and stellar and planetary obliquities, unlike other models which are only valid to a given order in the eccentricity, or for small (or zero) orbital inclinations (Goldreich & Soter 1966; Jackson et al. 2008a; Hut 1981). Using the secular evolution equations allows us to perform integrations quickly that represent dynamical evolution over billions of years. The full set of equations is presented in Appendix A in a form which is straightforward to numerically integrate. These equations have been written in such a way as to eliminate references to the basis vectors chosen in their representation, since the eccentricity basis vector is undefined for a circular orbit. In this form, the equations are regular at  $e = 0$ , unlike those in Eggleton & Kiseleva-Eggleton (2001) and Mardling & Lin (2002).

## 4 MAGNETIC BRAKING

Observations of solar-type stars have shown that the mean stellar rotational velocity decreases with time (Skumanich 1972), following the relation  $\Omega \propto t^{-1/2}$ , where  $t$  is the main-sequence age. This is the empirical Skumanich relation, and can be interpreted as telling us that solar-type stars have been undergoing continuous spin-down since they first started on the main sequence. Magnetic braking by a magnetised outflowing wind has long been recognised as an important mechanism for the removal of angular momentum from rotating stars (Weber & Davis 1967), and such a mechanism seems able to explain most of the observed stellar spin-down (Barnes 2003).

Although the Skumanich law is well established for stars with rotational velocities in the range  $1 - 30 \text{ km s}^{-1}$ , it overestimates the spin-down rates of stars up to  $t \sim 10^8$  yrs, and thus cannot explain the presence of fast rotators in the Pleiades (Ivanova & Taam 2003). As a resolution to this problem it has been suggested that the angular momentum loss rate for high rotation rates could be reduced, as a result of the saturation of the stellar dynamo (MacGregor & Brenner 1991), or alternatively due to a reduction in the number of open field lines in a complex magnetic field topology (Taam & Spruit 1989). These and similar approaches lead to modified models of the magnetic braking torque for fast rotators, and several such models have been proposed (e.g. Ivanova & Taam 2003; Holzwarth & Jardine 2005). Nevertheless, Barnes (2003) finds that the Skumanich relation is remarkably accurate at modelling the spin-down of Sun-like stars that are not rapid rotators, so to a first approximation, a magnetic braking torque based on the empirical Skumanich law is best for our purposes.

Here we include the effects of magnetic braking in the tidal evolution equations, through the inclusion of the Verbunt & Zwaan (1981) braking torque, with the particular coefficients of Dobbs-Dixon et al. (2004), as follows (see Appendix A)

$$\dot{\omega}_{\text{mb}} = -\alpha_{\text{mb}} \Omega_1^2 \boldsymbol{\Omega}_1, \quad (1)$$

where  $\alpha_{\text{mb}} = 1.5 \times 10^{-14} \gamma$  yrs.  $\gamma$  is a correction factor for F-dwarfs, which takes the value 0.1 for an F dwarf, but is unity for a G or K dwarf. We can also define a magnetic braking timescale  $\tau_{\text{mb}} \equiv \frac{\Omega_1}{\dot{\omega}_{\text{mb}}} = \frac{1}{\alpha_{\text{mb}}} \frac{1}{\Omega_1^2}$ , which is  $\sim 10^{10}$  yrs for the Sun.

## 5 ANALYSIS OF THE EFFECTS OF MAGNETIC BRAKING ON TIDAL EVOLUTION FOR A SIMPLIFIED SYSTEM

### 5.1 Circular, coplanar orbit with magnetic braking

We first study the effects of magnetic braking on a simplified system of a circular, coplanar orbit under the influence of only the tide that is raised on the star by the planet, and magnetic braking. We have neglected the tide in the planet here since the moment of inertia of the planet is much smaller than that of star and the orbit (i.e.  $I_2 \ll I_1 \sim m_2 a^2$ ), so to a first approximation we can neglect the effects of planetary spin; in any case the planetary spin is expected to synchronize rapidly with the orbit. The following set of dimensionless equations can be derived from the full set of equations in Appendix A:

$$\frac{d\tilde{\Omega}}{d\tilde{t}} = \tilde{n}^4 \left( 1 - \frac{\tilde{\Omega}}{\tilde{n}} \right) - A \tilde{\Omega}^3, \quad (2)$$

$$\frac{d\tilde{n}}{d\tilde{t}} = 3 \tilde{n}^{\frac{16}{3}} \left( 1 - \frac{\tilde{\Omega}}{\tilde{n}} \right), \quad (3)$$

where we have normalised the stellar spin frequency  $\Omega_1$  and orbital mean motion  $n$  to the orbital frequency at the stellar surface, together with a factor  $C^{3/4}$ .  $C$  is the ratio of the orbital angular momentum of a mass  $m_2$  in an orbit with semi-major axis equal to the stellar radius  $R_1$ , to the spin angular momentum of an equally rapidly rotating star of radius

$R_1$ , mass  $m_1$  and dimensionless radius of gyration  $r_{g1}$ . The reduced mass is  $\mu = \frac{m_1 m_2}{m_1 + m_2}$ .  $C$  is important for classifying the stability of the equilibrium curve  $\tilde{\Omega} = \tilde{n}$  in the absence of magnetic braking, and it can be shown from energy and angular momentum considerations that this equilibrium is stable if  $\tilde{n} \leq 3^{-\frac{3}{4}}$  – equivalent to the statement that no more than a quarter of the total angular momentum can be in the form of spin angular momentum for stability (Hut 1980). We have thus defined the following dimensionless quantities:

$$\tilde{\Omega} = \Omega_1 \left( \frac{R_1^3}{Gm_{12}} \right)^{\frac{1}{2}} C^{-\frac{3}{4}},$$

$$\tilde{n} = n \left( \frac{R_1^3}{Gm_{12}} \right)^{\frac{1}{2}} C^{-\frac{3}{4}},$$

$$C = \frac{\mu R_1^2}{I_1} = \frac{\mu}{r_{g1}^2 m_1},$$

$$\tilde{t} = \left( \frac{Gm_{12}}{R_1^3} \right)^{\frac{1}{2}} \left( \frac{9}{2Q'_1} \right) \left( \frac{m_2}{m_1} \right) C^{\frac{13}{4}} t,$$

$$A = \alpha_{\text{mb}} \left( \frac{Gm_{12}}{R_1^3} \right)^{\frac{1}{2}} \left( \frac{2Q'_1}{9} \right) \left( \frac{m_1}{m_2} \right) C^{-\frac{7}{4}}.$$

There is only one parameter ( $A$ ) that completely characterises the solution in the  $(\tilde{n}, \tilde{\Omega})$ -plane, and its value may be estimated as

$$A \simeq 100 \gamma \left( \frac{Q'_1}{10^6} \right),$$

for a Jupiter–mass planet orbiting a Sun–like star undergoing magnetic braking (with standard  $\alpha_{\text{mb}}$  and with  $Q' = 10^6$ ). The size of this term shows that in general magnetic braking dominates the stellar spin evolution. Note that in the absence of magnetic braking ( $A = 0$ ), Eqs. 2 and 3 do not contain reference to the masses of the star and planet or to the tidal  $Q'$  of the star. The parameter  $A$ , together with the initial conditions  $(\tilde{n}_0, \tilde{\Omega}_0)$ , completely determines the evolution.

We plot some solutions on the  $(\tilde{n}, \tilde{\Omega})$ -plane in Fig. 1 by integrating Eqs. 2 and 3 for various initial conditions. Fig. 1 shows two phase portrait plots, which show the general qualitative behaviour of the solutions to Eqs. 2 and 3, for a given value of the parameter  $A$ . The arrows on each curve show the direction of time evolution from the initial state. For prograde orbits we restrict ourselves to studying the region,  $0 \leq \tilde{n} \leq 10, 0 \leq \tilde{\Omega} \leq 10$ , in the  $(\tilde{n}, \tilde{\Omega})$ -plane. This is because  $\Omega_1 = \sqrt{Gm_{12}/R_1^3}$  corresponds to stellar breakup velocity and  $n \geq \sqrt{Gm_{12}/R_1^3}$  means that the planet would be orbiting at, or beneath, the stellar surface. For a HJ with a mass of  $M_J$  orbiting a star of mass  $M_\odot$ ,  $C \sim 0.01$ , so  $\tilde{n} \simeq 10$  corresponds to an orbital semi-major axis of  $a \simeq 0.01$  AU, and  $\tilde{n} \simeq 0.1$  corresponds to  $a \simeq 0.2$  AU, so these plots represent the full range of orbits of the HJs. The top plot in Fig. 1 is for  $A = 100$ , which corresponds to canonical magnetic braking for a G/K star ( $\gamma = 1$ ) and  $Q'_1$  of  $10^6$ .

In the absence of magnetic braking ( $A = 0$ ) we recover the standard tidal evolution equations for a coplanar, circular orbit. These have been well studied in the literature (e.g. Counselman 1973; Hut 1981). These equations have an equilibrium of coplanarity and corotation i.e.  $i = 0$  and  $\tilde{\Omega} = \tilde{n}$ , where the orbital inclination (or stellar obliquity)  $i$  is de-

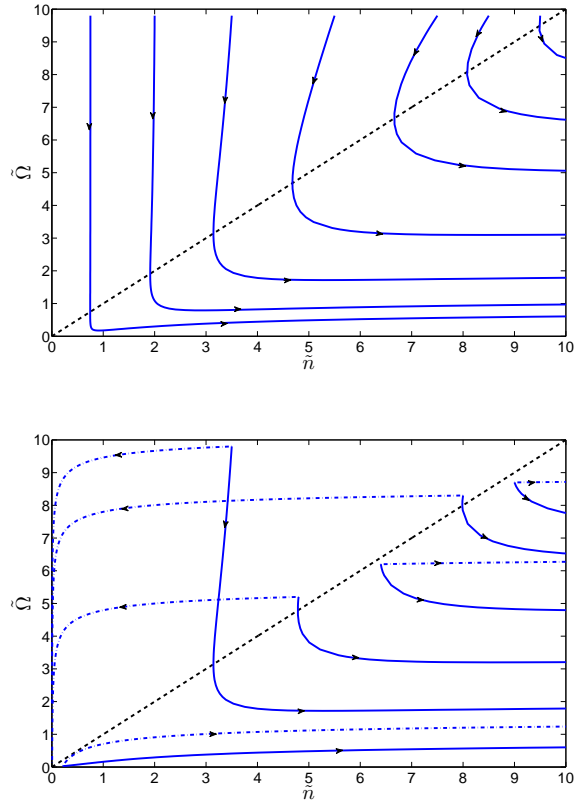


**Figure 1.**  $(\tilde{n}, \tilde{\Omega})$ -plane with  $A = 100$  for a HJ orbiting a Sun-like star. The diagonal dashed line in each plot corresponds to corotation ( $\tilde{\Omega} = \tilde{n}$ ). Top: magnetic braking spins the star down so that the planet finds itself inside corotation, where the sign of the tidal torque changes, and planet is subject to tidally induced orbital decay. For an initially high  $\tilde{n}$  outside corotation tidal friction efficiently transfers angular momentum from spin to orbit, which pushes the planet outwards. Bottom: Solutions with the same initial conditions are plotted with and without magnetic braking for a HJ around a solar-type star, with dot-dashed lines having  $A = 0$  and solid lines have  $A = 100$ . The dot-dashed lines are also curves of constant total angular momentum. This shows that the inclusion of magnetic braking is extremely important in determining the secular evolution of the system, and its absence results in a very different evolutionary history unless  $\tilde{\Omega} \ll \tilde{n}$  in the initial state.

fined by  $\cos i = \hat{\Omega}_1 \cdot \hat{\mathbf{h}}$  and  $i \geq 0$ . The system will approach this equilibrium if both the spin angular momentum is less than a quarter of the total angular momentum, and the total angular momentum exceeds some critical value (Hut 1980; Greenberg 1974). With no braking, orbits initially outside corotation ( $\tilde{\Omega} > \tilde{n}$ ) are not subject to tidally induced orbital decay, and asymptotically approach a stable equilibrium  $\tilde{\Omega} = \tilde{n}$  for  $\tilde{n} \leq 3^{-\frac{3}{4}}$ . Orbits initially inside corotation can evolve in two different ways, depending on the stability of the equilibrium state on the solution's closest approach to  $\tilde{\Omega} = \tilde{n}$ . If  $\frac{d\tilde{\Omega}}{dt} > \frac{d\tilde{n}}{dt} > 0$  near corotation, then  $\tilde{n} \leq 3^{-\frac{3}{4}}$ , and the equilibrium state is locally stable (though no such curves are plotted in Fig. 1, since they occur only in the far bottom left of the plot, near the origin). This is when the corotation radius moves inwards faster than the orbit shrinks due to tidal friction, which can result in a final stable equilib-

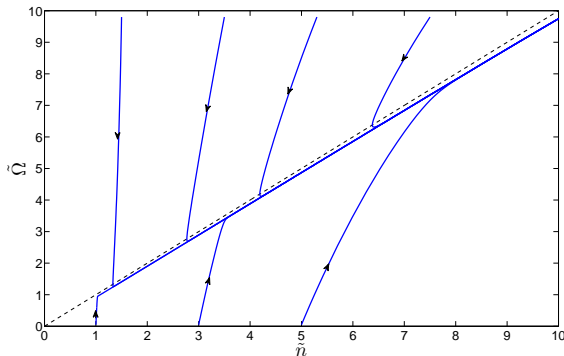


**Figure 2.**  $(\tilde{n}, \tilde{\Omega})$ -plane showing the effects of reducing the stellar mass fraction participating in angular momentum exchange with the orbit while the braking rate is unchanged, as has been proposed for an F star like  $\tau$  Boo.  $A = 100$ ,  $\epsilon_* = 10^{-2}$

rium state for the system if the corotation radius “catches up” with the planet. On the other hand, orbits inside corotation for which this condition is not satisfied are subject to tidally induced orbital decay, since tidally induced angular momentum exchange enhances the difference between  $\tilde{\Omega}$  and  $\tilde{n}$ , which leads to further orbital evolution, and the spiralling in of the planet. This evolution can be seen from the dot-dashed lines in the bottom plot in Fig. 1.

Including magnetic braking ( $A \neq 0$ ) means that  $\tilde{\Omega} = \tilde{n}$  is no longer an equilibrium state, and the total angular momentum of the system is not conserved. For an orbit initially not subject to spiralling into the star via tidal transfer of angular momentum from orbit to spin ( $\tilde{\Omega} \geq \tilde{n}$ ) we see from the top of Fig. 1, that magnetic braking will spin the star down so that the planet finds itself inside the corotation radius of the star. Passing through corotation changes the sign of the tidal torque and causes the planet to spiral into the star. Note that, if we ignore the age of the system, any bound orbit will eventually decay in a finite time since the system has no stable equilibrium. The effect of magnetic braking is to increase the minimum semi-major axis at which the orbit is not subject tidally induced orbital decay over the nuclear lifetime of the star.

This means that an initially rapidly rotating G-type star hosting a close-in Jupiter mass companion will lose significant spin angular momentum through magnetic braking (over a time  $\sim \tau_{\text{mb}}$ ). During this stage of spin-down the spin frequency of the star may temporarily equal the orbital frequency of its close-in planet, but the rate of angular momentum loss through magnetic braking will exceed the tidal rate of transfer of angular momentum from orbit to spin. The stellar spin continues to drop well below synchronism until the efficiency of transfer of tidal angular momentum from orbit to spin can compensate or overcompensate for the braking. If  $\frac{d\tilde{\Omega}}{dt} > \frac{d\tilde{n}}{dt} > 0$  inside corotation, then tides will act to spin up the star, though the timescale for this to cause significant spin-up may be much longer than the stellar lifetime, and this only occurs if the orbit has sufficient angular momentum to noticeably spin up the star. Otherwise, the planet continues to spiral inwards once it moves inside corotation, and  $\tilde{\Omega} \simeq \text{const.}$

So far we have considered the whole star to participate in tidal angular momentum exchange with the orbit. For an F-dwarf (like  $\tau$  Boo), it has been proposed that only the outer convective envelope (of mass fraction  $\sim \epsilon_*$ ) participates in angular momentum exchange with the orbit (Marcy et al. 1997; Dobbs-Dixon et al. 2004; Donati et al. 2008). If the core and envelope of such a star can decouple, then tides would only have to spin up the outer layers of the star, which would reduce the spin-up time by  $\sim \epsilon_*$ . In this case the system could remain in a state with  $\tilde{\Omega} \simeq \tilde{n}$  just inside corotation, with the resulting torque on the orbit small. This may explain the spin-orbit synchronism of stars such as  $\tau$  Boo, as noted by Dobbs-Dixon et al. (2004). Fig. 2 shows the phase plane for a simplified system in which the moment of inertia of the star acted on by tides is reduced by a factor  $\epsilon_* \sim 10^{-2}$ , but the braking rate is unchanged i.e. we multiply the first term on the right-hand side of Eq. 2 by  $\epsilon_*^{-1}$ . Note that this may be too simple a model to describe such core-envelope decoupling, and we have ignored associated changes to the braking rate.

## 5.2 Extending the analysis to inclined circular orbits

We can extend the simplified system of equations analysed in the previous section to arbitrary inclination ( $i$ ) of the orbital plane with respect to the equatorial plane of star:

$$\frac{d\tilde{\Omega}}{dt} = \tilde{n}^4 \left[ \cos i - \frac{\tilde{\Omega}}{2\tilde{n}} (1 + \cos^2 i) \right] - A \tilde{\Omega}^3, \quad (4)$$

$$\frac{d\tilde{n}}{dt} = 3 \tilde{n}^{\frac{16}{3}} \left[ 1 - \frac{\tilde{\Omega}}{\tilde{n}} \cos i \right], \quad (5)$$

$$\frac{di}{dt} = -\tilde{n}^4 \tilde{\Omega}^{-1} \sin i \left[ 1 - \frac{\tilde{\Omega}}{2\tilde{n}} (\cos i - \tilde{n}^{\frac{1}{3}} \tilde{\Omega}) \right], \quad (6)$$

For small inclination, Eq. 6 reproduces Eq. 13 from Hut (1981), with the exception that we have used a constant  $Q'_1$  rather than a constant time-lag in the equations (i.e. replace time lag  $\tau$  by  $\frac{1}{2} \frac{3}{2k_1 n Q'_1}$ , and note that  $k_1$  is twice the apsidal motion constant of the star).

From Eq. 5 the orbit begins to decay if

$$\tilde{\Omega} \cos i < \tilde{n}, \quad (7)$$

which is always satisfied for a retrograde orbit ( $i \geq 90^\circ$ ). This is just a generalisation of the corotation condition  $\tilde{\Omega} = \tilde{n}$  to a non-coplanar orbit. The inclination grows if

$$\tilde{\Omega} > \tilde{\Omega}_{\text{crit}} = 2\tilde{n} \left( \cos i - \tilde{n}^{\frac{1}{3}} \tilde{\Omega} \right)^{-1}, \quad (8)$$

where we have assumed the quantity in brackets is positive i.e.  $\cos i > \tilde{n}^{\frac{1}{3}} \tilde{\Omega}$ . This agrees with the condition from Hut (1981) when  $i \sim 0$ . For sufficiently close-in orbits that tidal friction is important, magnetic braking will rapidly spin down the star such that this condition is not satisfied, so we can safely conclude that the inclination is not likely to grow appreciably by tidal friction. When this condition is not satisfied, the inclination decays to zero, on a timescale  $\tau_i$  (see next section). Note that  $i = 180^\circ$  is an unstable equilibrium value of the inclination.

In the absence of magnetic braking we recover the evolution considered by Greenberg (1974), so we will now con-

centrate on the inclusion of magnetic braking. The top figure in Fig. 3 plots the  $(\tilde{n}, \tilde{\Omega})$ -plane for  $A = 10$  for an initial inclination of  $i = 90^\circ$ . A smaller value of  $A$  is chosen over the previous section in order to show the effects of tides more clearly, since reducing  $A$  is equivalent to reducing  $Q'$ . The evolution of  $i$  is not plotted (and will in general be different for each curve), but is found to decay once the stellar spin decays sufficiently that Eq. 8 is not satisfied. The bottom figure in Fig. 3 shows the effect of increasing the inclination in steps to illustrate the behaviour as  $i$  is increased, on various curves with otherwise the same initial conditions, with  $A = 10$ . The orbit begins to decay for smaller  $\tilde{n}$ , and decays at a faster rate as  $i$  is increased. This peaks for a perfectly retrograde orbit ( $i = 180^\circ$ ), with anti-parallel spin and orbit, where the rates of change of spin and orbital angular frequencies are maximum. Fig. 3 shows that the orbit generally begins to decay outside corotation, once  $\tilde{\Omega} \cos i < \tilde{n}$ . This has implications for the tidal evolution of close-in planets on inclined orbits, in that if this condition is satisfied, the planet will be undergoing tidally induced orbital decay – though the inspiral time may be longer than the expected stellar lifetime.

In this section we have seen that magnetic braking can only be reasonably neglected for a coplanar orbit when  $\Omega \ll n$ . For an inclined orbit, this condition must be generalised to  $\Omega \cos i \ll n$  – obvious from Eq. 5. Neglecting  $\dot{\omega}_{\text{mb}}$  for stars for which this condition is not satisfied can result in a qualitatively different evolution, as already seen in Fig. 1(b) for a coplanar orbit.

## 6 TIDAL EVOLUTION TIMESCALES

It is common practice to interpret the effects of tidal evolution in terms of simple timescale estimates. The idea behind these is that if the rate of change of a quantity  $X$  is exponential, then  $\dot{X}/X$  will be a constant, so we can define a timescale  $\tau_X = X/\dot{X}$ . If  $\dot{X}/X \neq \text{const}$ , then these may not accurately represent the evolution. Here we reproduce the timescales that can be derived from the equations in Appendix A.

A tidal inspiral time can be calculated from the equation for  $\dot{a}$ , by considering only the effects of the tide raised on the star by the planet (not unreasonable since  $I_2 \ll I_1 \sim m_2 a^2$ ). Here  $\dot{a}/a \sim a^{-13/2} \neq \text{const}$ , so a more accurate estimate of the inspiral time for a circular coplanar orbit is

$$\tau_a \equiv -\frac{2}{13} \frac{a}{\dot{a}} \simeq 12.0 \text{ Myr} \left( \frac{Q'_1}{10^6} \right) \left( \frac{m_1}{M_\odot} \right)^{\frac{8}{3}} \left( \frac{M_J}{m_2} \right) \left( \frac{R_\odot}{R_1} \right)^5 \left( \frac{P}{1\text{d}} \right)^{\frac{13}{3}} \left( 1 - \frac{P}{P_*} \right)^{-1}$$

Here  $P$  and  $P_*$  are the orbital and stellar spin periods, respectively. We have already seen in §5 that it is unreasonable to assume that  $\Omega$  is fixed unless  $\Omega \ll n$ , due to magnetic braking.

If the orbit is inside corotation, angular momentum will be transferred from the orbit to the spin of the star, giving a tidal spin-up time of

$$\tau_{\Omega_1} \equiv -\frac{\dot{\Omega}_1}{\Omega_1} \simeq \frac{13\tau_a}{2\alpha},$$

where  $\alpha = \frac{\mu h}{I\Omega}$  is the ratio of orbital to spin angular momentum. For the HJ problem,  $\tau_{\Omega_1} \geq \tau_a$  since  $\alpha \sim O(1)$ ,

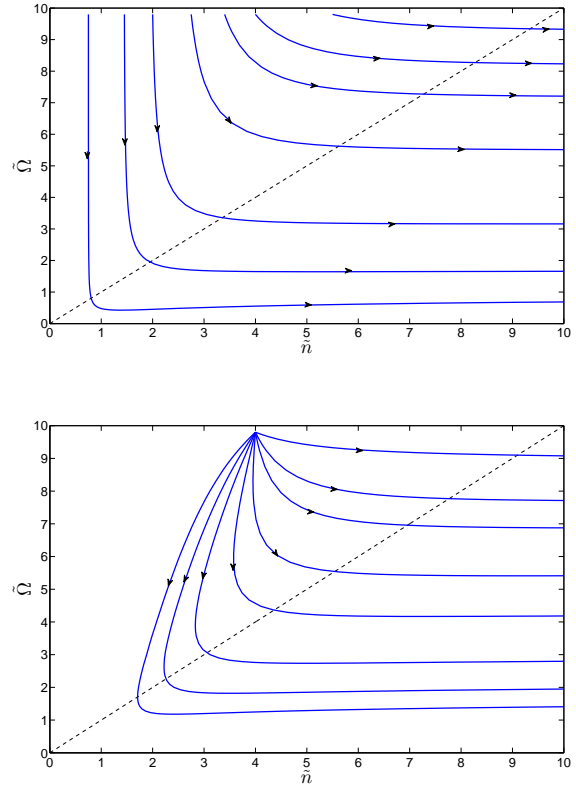


**Figure 3.** Top:  $(\tilde{n}, \tilde{\Omega})$ -plane for an orbit with an initial  $i = 90^\circ$ , with  $A = 10$ , where the dashed line corresponds to  $\tilde{\Omega} = \tilde{n}$ . This is similar to Fig. 1(a) for a circular orbit, except that the orbit decays once  $\tilde{\Omega} \cos i < \tilde{n}$ , which can occur above the dashed line in contrast with the circular case. The evolution of  $i$  is not plotted, and is in general different for each curve, but is found to decay once the stellar spin drops below that given by Eq. 8. Bottom: various initial inclinations, with  $A = 10$ , where the dashed line corresponds to  $\tilde{\Omega} = \tilde{n}$ . The bottom trajectory has  $i = 0$ , and the inclination is increased in steps towards the top curve, which has  $i = 180^\circ$ , to illustrate the behaviour. Note that orbits with larger initial  $i$  decay for smaller  $\tilde{n}$ , once  $\tilde{\Omega} \cos i < \tilde{n}$  is satisfied.

which neglects the spin-down effects of magnetic braking. The planetary spin  $\Omega_2$  will tend to synchronise much faster, since the moment of inertia of the planet is much less than that of the orbit (by  $\sim 10^5$ ), and will not be considered further i.e. we assume  $\Omega_2 = n$ .

A circularisation time can be derived from the equation for  $\dot{e}$ , and is given for a coplanar orbit by

$$\tau_e \equiv -\frac{e}{\dot{e}} \simeq 16.8 \text{ Myr} \left( \frac{Q'_1}{10^6} \right) \left( \frac{m_1}{M_\odot} \right)^{\frac{8}{3}} \left( \frac{M_J}{m_2} \right) \left( \frac{R_\odot}{R_1} \right)^5 \left( \frac{P}{1\text{d}} \right)^{\frac{13}{3}} \times \left[ \left( f_1(e^2) - \frac{11}{18} \frac{P}{P_*} f_2(e^2) \right) + \beta \left( f_1(e^2) - \frac{11}{18} f_2(e^2) \right) \right]^{-1}$$

where we have included both the stellar and planetary tides, as these have been shown to both contribute to the tidal evolution of  $e$  (Jackson et al. 2008a). Note that  $\dot{e}/e \sim \text{const}$  only if  $P \sim \text{const}$  and  $e \ll 1$ , where  $f_{1,2}(e^2) \simeq 1$ . The factor

$$\beta = \frac{Q'_2}{Q'_1} \left( \frac{m_1}{m_2} \right)^2 \left( \frac{R_2}{R_1} \right)^5 \sim 10 \frac{Q'_2}{Q'_1}$$



for the HJ problem.

If the orbital and stellar equatorial planes are misaligned, then dissipation of the tide raised on the star by the planet would align them on a timescale

$$\begin{aligned} \tau_i &\equiv -\frac{i}{\frac{di}{dt}} \\ &\simeq 70 \text{ Myr} \left(\frac{Q'_1}{10^6}\right) \left(\frac{m_1}{M_\odot}\right) \left(\frac{M_J}{m_2}\right)^2 \left(\frac{R_\odot}{R_1}\right)^3 \left(\frac{P}{1\text{d}}\right)^4 \\ &\quad \times \left(\frac{\Omega_1}{\Omega_0}\right) \left[1 - \frac{P}{2P_*} \left(1 - \frac{1}{\alpha}\right)\right]^{-1} \end{aligned}$$

where we have assumed that the orbit is circular and made the small  $i$  approximation. We take  $\Omega_0 = 5.8 \times 10^{-6} \text{s}^{-1}$ , which corresponds to a spin period of  $\sim 12.5$  d.

The validity of these timescales to accurately represent the tidal evolution of the orbital and rotational elements is an important subject of study, since these timescales are commonly applied to observed systems. In a recent paper, Jackson et al. (2008a) found that it is essential to consider the coupled evolution of  $e$  and  $a$  in order to accurately model the tidal evolution, and that both the stellar and planetary tides must be considered. They showed that the actual change of  $e$  over time can be quite different from simple circularisation timescale considerations, due to the coupled evolution of  $a$ . In the following we will consider the validity of the spin-orbit alignment timescale to accurately model tidal evolution of  $i$ .

## 7 NUMERICAL INTEGRATIONS OF THE FULL EQUATIONS FOR AN INCLINED ORBIT

We perform direct numerical integrations of the equations in Appendix A with a 4th/5th order Runge-Kutta scheme with adaptive stepsize control, using a scheme with Cash-Karp coefficients similar to that described in Press et al. (1992). Our principal aim is to study inclination evolution and to determine the accuracy of the spin-orbit alignment timescale  $\tau_i$  for close-in planets.

We choose a “standard” system of a HJ in orbit around an FGK star. We have  $m_1 = M_\odot$ ,  $m_2 = M_J$ ,  $R_1 = R_\odot$ ,  $R_2 = R_J$ , and we modify<sup>2</sup>  $a$ ,  $i$ ,  $e$ . We choose the initial ratio  $\Omega_1/n = 10$ , and include magnetic braking in all simulations, setting  $\gamma = 1$  unless stated otherwise. We choose  $Q'_1 = Q'_2 = 10^6$ , and  $\Omega_2/n = 1$  unless stated otherwise. The dimensionless radii of gyration are chosen to be  $r_{g1}^2 = 0.076$  and  $r_{g2}^2 = 0.261$ , which are values appropriate for polytropic stellar and planetary models with respective indices 3 and 1.

### 7.1 Inclusion of magnetic braking and the importance of coupled evolution of $a$ and $i$

For a prograde orbit ( $i < 90^\circ$ ) initially outside corotation,  $\dot{\omega}_{\text{mb}}$  rapidly spins the star down sufficiently to ensure that inclination is not excited through tidal friction (so that Eq. 8

is not satisfied), and the inclination begins to decay. Subsequent spin-down moves the orbit-projected corotation radius beyond the orbit of the planet (so that  $\Omega \cos i < n$ ), and the resulting tidal inspiral accelerates as the difference between  $\Omega \cos i$  and  $n$  is enhanced. The associated reduction in  $a$  increases the rate of stellar spin-orbit alignment. Thus the inclusion of  $\dot{\omega}_{\text{mb}}$  increases the rate of alignment, and reduces  $\tau_i$  from the simple estimate, which ignores magnetic braking and coupled  $a$  and  $i$  evolution.

The effect of  $\dot{\omega}_{\text{mb}}$  on a retrograde orbit ( $i \geq 90^\circ$ ) is qualitatively different. A retrograde orbit is always subject to tidally induced inspiral since  $\Omega \cos i < n$  for all  $i \geq 90^\circ$ .  $\dot{\omega}_{\text{mb}}$  acts to reduce  $\Omega$ , thereby reducing the difference  $|\Omega \cos i - n|$ , making the tidal torque smaller. This acts to *increase* the timescale for alignment of the stellar spin and orbit, though the effect is found to be small.

The most important effect of including  $\dot{\omega}_{\text{mb}}$  is simply that of reducing the stellar spin sufficiently so that  $\Omega \cos i < n$ , where the semi-major axis can then decay through tidal friction. As  $a$  subsequently decreases, the tidal torque increases, resulting in a faster inclination decay rate.  $\dot{\omega}_{\text{mb}}$  can only be neglected if  $|\Omega \cos i| \ll n$ . If the orbit is already highly inclined, such as  $i \geq 90^\circ$ , then the inclusion of magnetic braking is not so important, since  $\Omega \cos i < n$  regardless of the spin rate.

For an orbit initially at  $a = 0.05$  AU, the simple estimate of the stellar spin-orbit alignment timescale gives  $\tau_i \simeq 2.0 \times 10^{10}$  yrs. Fig. 4 shows the evolution of  $i$  and  $a$  for various initial inclinations for an orbit at  $a = 0.05$  AU and  $a = 0.08$  AU respectively. The outer orbit  $a$  changes only slightly over 10 Gyr, and  $i$  evolves as expected from the simple estimate of  $\tau_i \simeq 3.0 \times 10^{11}$  yrs. The inner orbit, on the other hand, is subject to tidally induced orbital decay, with an inspiral time of 1–3 Gyr, and this reduction in  $a$  increases the rate of inclination evolution. This highlights the importance of considering coupled evolution of  $a$  and  $i$ , especially for large initial inclinations, where inspiral occurs for higher stellar spin rates. The difference between the simple estimate of  $\tau_i$  and the true timescale can be up to an order of magnitude different for orbits whose  $a$  changes appreciably.

### 7.2 Inclined and eccentric orbits

Jackson et al. (2008a) already highlighted the importance of coupled  $a$  and  $e$  evolution for a coplanar orbit. We will now consider how  $e$  might affect  $i$  evolution for a non-coplanar orbit, which is the subject of this section.

A nonzero eccentricity reduces the pericentre distance  $r_p = a(1 - e)$ , which increases the tidal torque over a circular orbit, since tidal torque  $\sim r^{-6}$ . Although the planet would spend less time near pericentre, the torque there is much greater, so dominates the orbit-averaged torque. We therefore expect the stellar spin-orbit alignment time to be reduced as we increase  $e$ . In addition, we expect that an orbit at large  $e$  would more strongly affect the rate of alignment over a circular orbit, than one at large  $i$  would over a coplanar orbit, because  $e$  reduces  $r_p$ , whereas  $i$  only changes the difference  $(\Omega \cos i - n)$ . The tidal torque  $\sim r^{-6}(\Omega \cos i - n)$ , which depends more strongly on  $r$  than  $\Omega$ . This behaviour can be seen in Figs. 4(d) and 5(b) which shows that the ratios of stellar spin-orbit alignment times for an orbit with

<sup>2</sup> We take  $\Omega_1 \cdot \mathbf{e} = 0$ , though this need not be assumed. We find negligible difference between integrations for which  $\Omega_1 \cdot \mathbf{e} = 0$  and  $\Omega_1 \cdot \mathbf{e} \neq 0$



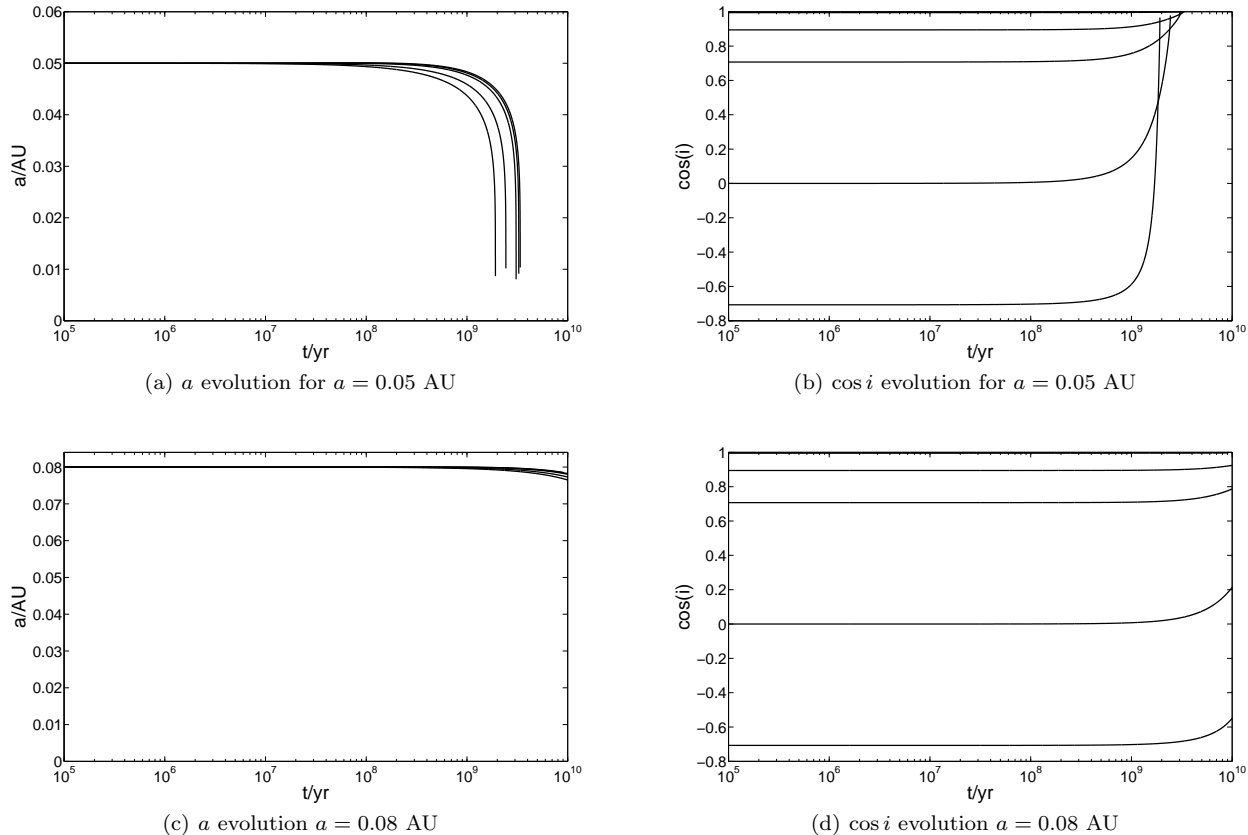


**Figure 4.** Tidal evolution for a circular, inclined orbit at  $a = 0.05$  AU and  $a = 0.08$  AU, with various initial inclinations:  $i = 6^\circ, 26^\circ, 45^\circ, 90^\circ, 180^\circ$ . (a) and (c) show their respective semi-major axis evolutions (with the highest inclination orbit decaying first – the bottom curve – and the lowest inclination orbit decaying last – the top curve), and (b) and (d) show the respective inclination evolution for these systems. The outer orbit  $a$  changes only slightly over 10 Gyr, and  $i$  evolves as expected from simple estimates of  $\tau_i$ . The inner orbit, on the other hand, is tidally shrunk, and this reduction in  $a$  means that the true evolution is much faster than the simple timescale estimates predict. This highlights the importance of considering coupled evolution of  $a$  and  $i$ .

small  $i$  and large  $i$  is  $\sim O(1)$ , whereas the ratios of stellar spin-orbit alignment times for an orbit with small  $e$  and large  $e$  can be up to several orders of magnitude.

From Fig. 5 we can compare the simple estimate of  $\tau_i \simeq 3.0 \times 10^{11}$  yrs for an orbit at  $a = 0.08$  AU, with the coupled evolution of the orbital and rotational elements from integration of the full equations. We see that the simple estimate gives a misleadingly long stellar spin-orbit alignment time compared with that obtained from integrating the full equations in cases where  $e$  is initially non-negligible – as a result of the strong functions of the eccentricity in this model of tidal friction (see Appendix A). This confirms the conclusion of Jackson et al. (2008a), in that it is essential to consider coupled evolution of  $a$  and  $e$  in order to determine an accurate system history. We also find that the associated changes in semi-major axis strongly affect stellar spin-orbit alignment. A marginally better estimate for  $\tau_i$  can be made by replacing the orbital period with the orbital period around periastron (equivalent to replacing  $a$  by  $r_p$ ), though this is still inadequate since it neglects evolution of  $a$ .

### 7.3 Discussion

For typical HJs, we find that the stellar spin-orbit alignment time is comparable to the inspiral time i.e.  $\tau_i \sim \tau_a$ . This means that if we observe a planet, then its survival implies that tides are unlikely to have aligned its orbit. For planets on an accelerating inspiral into the star, the rate of inclination evolution will have been much lower in the past. Therefore if we observe a planet well inside corotation ( $\Omega \cos i < n$ ), with a roughly coplanar orbit, we can assume that it must have started off similarly coplanar – unless we are lucky enough to be observing a planet on its final rapid inspiral into the star after it has undergone most of the evolution, where it is now in a very short-period orbit, close to being consumed.

We expect  $\tau_i \sim \tau_a$  when  $\alpha \ll 1$  – which is true for close-in terrestrial planets – since  $\Omega$  can be considered fixed, with the inclination changing only due to changes in  $\mathbf{h}$ . For typical values of  $\alpha \sim O(1)$  for HJs, the inclination changes due to rotations of both  $\Omega$  and  $\mathbf{h}$ , so the timescales are not exactly the same, but would be expected to be of the same order of magnitude.

Hut (1981) showed by considering only the tide in the star, that the stellar spin-orbit alignment timescale is longer

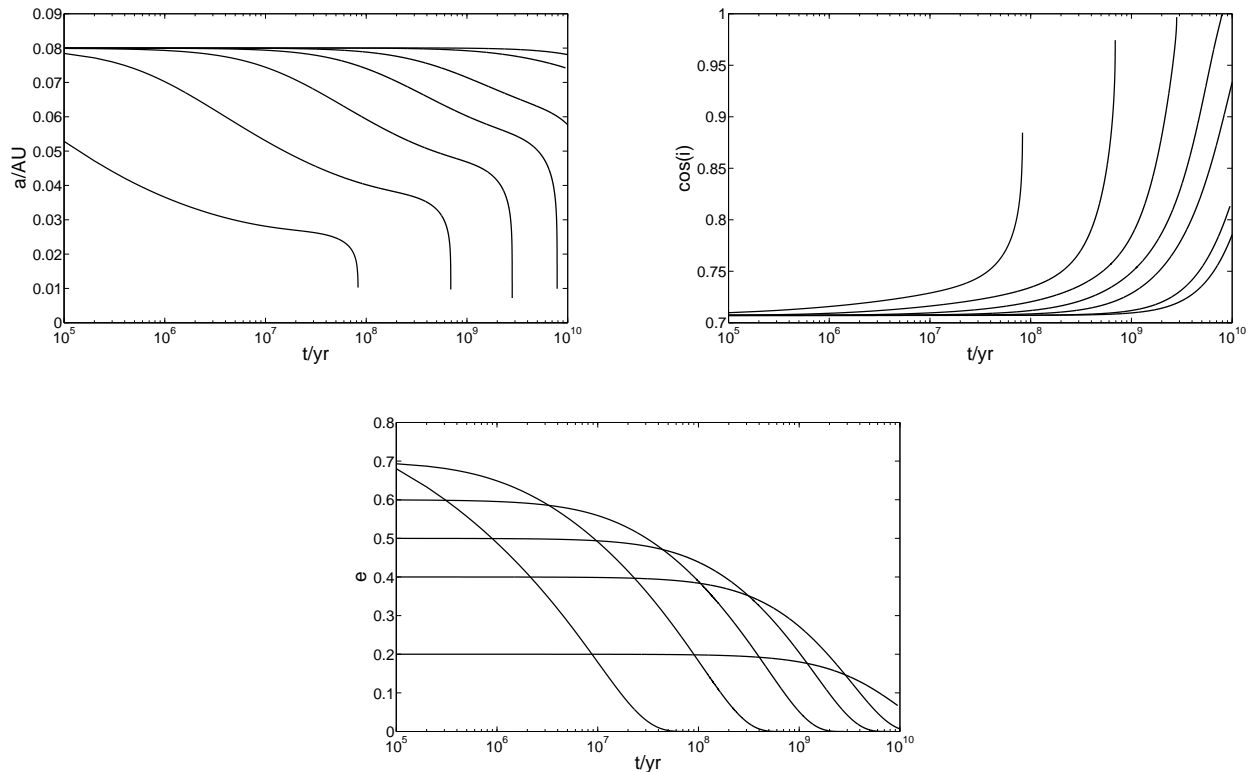


**Figure 5.** Top left: Semi-major axis evolution for an inclined orbit with initial  $i = 45^\circ$  at  $a = 0.08$  AU for various initial  $e$ , with  $e = 0, 0.2, 0.4, 0.5, 0.6, 0.7, 0.8$ . Top right and bottom: Inclination and eccentricity evolution for the same systems. Solutions with the smallest initial  $e$  have the smallest change in  $a$  and  $i$ . Solutions with the largest initial  $e$  undergo much more rapid tidal evolution (note that for  $e = 0.8$ ,  $e$  decays to less than 0.7 within  $10^5$  yrs) – curves can be distinguished by noting that the curves corresponding to the fastest evolution have the largest initial  $e$ . Increasing the eccentricity can be seen to reduce the inspiral time by up to several orders of magnitude over the circular case. In contrast, increasing the inclination in Fig. 4 only reduces the inspiral time by a factor  $\sim O(1)$  over a coplanar orbit. Also note that  $\tau_e < \tau_i$  for all integrations.

than the circularisation timescale ( $\tau_i > \tau_e$ ) unless  $\alpha > 6$ . This was based on exponential decay estimates for small  $e$  and  $i$ , but nevertheless holds for the systems integrated in this work, as can be seen from Fig. 5. This makes intuitive sense, since  $\alpha \sim O(1)$  means that spin angular momentum is important, and circularisation involves only a property of the orbit, whereas alignment involves both the spin and the orbit. For typical HJs  $\alpha < 6$ ; we therefore expect  $\tau_e < \tau_i$ , especially when the eccentricity damping effect of the tide in the planet is taken into account, which further enhances this inequality. The tide in the planet is completely negligible in changing the stellar obliquity since  $I_2 \ll I_1 \sim m_2 a^2$ .

This means that if an orbit is initially inclined and eccentric as a result of planet–planet scattering or Kozai migration into a short–period orbit, we would expect the orbit to become circular before it aligns with the spin of the star. We should therefore observe fewer eccentric orbits than inclined orbits, *if those systems start with a uniform distribution in  $e, i$ -space*. This also means that if we observe a close-in planet on a circular orbit with non-zero  $i$ , we cannot rule out a non-negligible eccentricity in the past.

## 8 APPLICATION TO OBSERVED SYSTEMS

### 8.1 An explanation of the misaligned spin and orbit of XO-3 b

The only system currently observed with a spin–orbit misalignment<sup>3</sup> is XO-3 (Hébrard et al. 2008; Johns-Krull et al. 2008), which has a sky–projected spin–orbit misalignment angle of  $\lambda \simeq 70^\circ \pm 15^\circ$ . This system has a very massive  $m_2 = 12.5 M_J$  planet on a moderately eccentric  $e = 0.29$ ,  $P = 3.2$  d orbit around an F-type star of mass  $m_1 = 1.3 M_\odot$ . Its age is estimated to be  $\tau_* \simeq (2.4 - 3.1)$  Gyr. Note that even if the star is rotating near breakup velocity ( $P_* \sim 1$  d), the planet is still subject to tidal inspiral, since  $P_* > P \cos i$  (where we henceforth assume  $i = \lambda$ , which may slightly *underestimate*  $i$ ). If we assume that the angle of inclination of the stellar equator to the plane of the sky is  $\sim 90^\circ$ , then  $P_* = 3.3$  d  $\sim P$  i.e.  $\Omega \sim n$ .

<sup>3</sup> This spin–orbit misalignment has been confirmed since the submission of the present paper by Winn et al. (2009), who find that the sky–projected spin–orbit misalignment angle  $\lambda = 37.3^\circ \pm 3.7^\circ$ , which is significantly smaller than that found by Hébrard et al. (2008). Nevertheless, our conclusions below should still be valid.

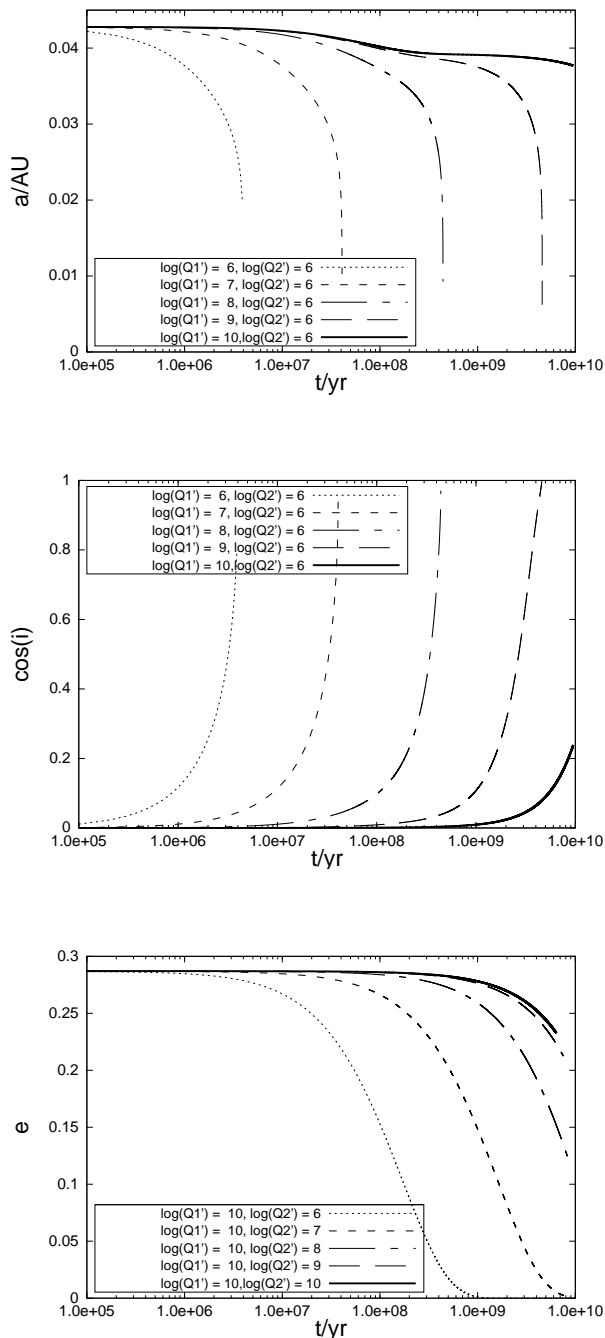


**Figure 6.** Tidal evolution of XO-3 b taking current values for the orbital properties of the system, except that  $\cos i = 90^\circ$  (not unreasonable since this roughly corresponds to the upper limit on  $\lambda$ , which in any case gives a lower bound on  $i$ ). Magnetic braking is included with  $\gamma = 0.1$ , and  $\Omega_1/n = 2$  initially (results do not depend strongly on this choice). From the top and middle plots we require  $Q'_1 \geq 10^{10}$  for the planet to survive for several Gyr, and maintain its high inclination. From the bottom plot we see that if  $Q'_1 \geq 10^{10}$ , we require  $Q'_2 \geq 10^8$  to maintain the current eccentricity for a few Gyr. Tidal dissipation in both the planet and star must therefore be weak to explain the current configuration of the system.

Hébrard et al. (2008) quote a stellar spin-orbit alignment timescale of  $\sim 10^{12}$  yr for this system, but we find that this is in error by  $\sim 10^5$ . We believe that the reason for this discrepancy is that their estimate was based on assuming that the spin-orbit alignment time for XO-3 b is the same as for HD17156 b (Narita et al. 2008; Cochran et al. 2008), which is a less massive planet on a much wider orbit. We find  $\tau_i \sim 30$  Myr (using the expression in §6) assuming  $Q'_1 = 10^6$  to align the whole star with the orbit. Circularisation time of  $\tau_e \sim 10$  Myr and the inspiral time is estimated to be  $\tau_a \sim 16$  Myr from simple estimates.

Integrations for this system are given in Fig. 6 for a variety of stellar and planetary  $Q'$  values. These integrations again highlight the importance of considering coupled evolution of the orbital and rotational elements, since timescales for tidal evolution can be quite different from the simple estimates given above. Indeed, the actual spin-orbit alignment time from integrating the full set of equations is about an order of magnitude smaller than that from the simple decay estimate, due to the semi-major axis evolution.

For the cases considered, the system can only survive and remain with its current inclination for  $\sim 3$  Gyr if  $Q'_1 \geq 10^{10}$ . An explanation for the survival and remnant orbital inclination of XO-3 b could therefore be the inefficiency tidal dissipation in the host star. The host star is an F-star of mass  $m_1 = 1.3 \pm 0.2 M_\odot$ , so it will contain a small convective core and a very thin outer convection zone (OCZ) separated by a radiative zone. Dissipation in the convective core will only weakly affect the tide, and dissipation in the radiation zone will also be weak (Zahn 2008). This is because internal inertia-gravity waves excited at the interface between convective and radiative regions cannot reach the photosphere, where they can damp efficiently, as supposed for high-mass stars. In addition, nonlinear effects due to geometrical concentration of the waves in the centre of the star cannot occur because the waves will reflect from the outer boundary of the inner convection zone well before they become nonlinear (Goodman & Dickson 1998; OL07).

We expect that most dissipation occurs in the OCZ of the star. A calculation of  $Q'$  for the dissipation of the equilibrium tide and inertial modes, in the thin OCZ, using a stellar model<sup>4</sup> appropriate for this star (note that the metallicity of the star is subsolar, with  $Z \sim 0.01$ ), was performed (see OL07; OL04 for details of the numerical method). It must be noted that these calculations involve uncertainties regarding the effective viscosity of turbulent convection, though the general trends in the results below (and in the next section) are likely to be quite robust. The results for the  $m = 0, 1, 2$  components of the tide are plotted in Fig. 7. In Appendix B, we show that a combination of the  $m = 0, 1, 2$  components of the tide are relevant for spin-orbit alignment and inspiral, and so we must calculate  $Q'$  for all components of the  $l = 2$  (quadrupolar) tide. The relevant tidal frequencies, assuming  $\Omega \sim n$  currently, would be those of integer  $\hat{\omega}/\Omega$ . However, since the angle of inclination of the stellar equatorial plane to the plane of the sky has not been determined, the relevant tidal frequencies cannot be calculated with any certainty. Nevertheless,  $Q' \geq 10^{10}$  for most tidal frequencies

<sup>4</sup> for which we use EZ Web at <http://shayol.bartol.udel.edu/~rhdt/ezweb/>

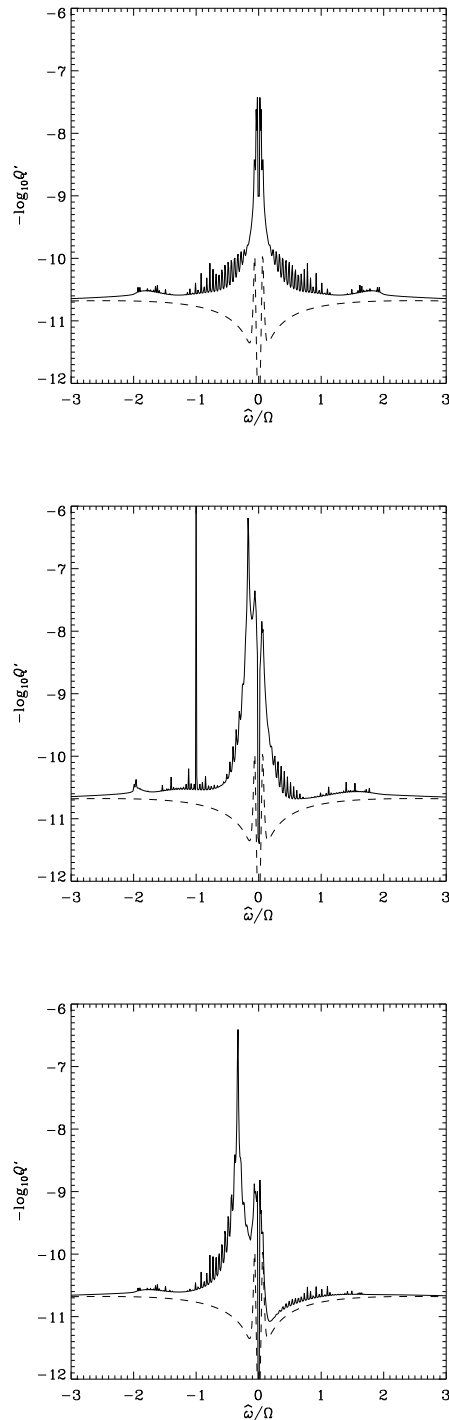


**Figure 7.** Tidal  $Q'$ -factor as a function of the ratio of tidal frequency to spin frequency  $\hat{\omega}/\Omega$ , from dissipation of the  $l = 2$ ,  $m = 0, 1, 2$  components respectively, of the equilibrium tide and dissipation of inertial modes in the OCZ of an F-type star (see OL07 for details of this calculation). This used a stellar model appropriate for XO-3 to model the convection zone. The dashed lines represent the effect of omitting the Coriolis force, and therefore inhibiting inertial waves. The prominent features in each figure (which occur for  $\hat{\omega}/\Omega = -1$  and  $-1/6$  for  $m = 1$  and  $\hat{\omega}/\Omega = -1/3$  for  $m = 2$ ) are Rossby waves, which are probably excited for tidal frequencies not relevant for the XO-3 system. For most tidal frequencies  $Q' \geq 10^{10}$ , which could explain the survival and remnant orbital inclination of XO-3 b.

for the host star XO-3. This can explain the survival and remnant inclination of XO-3 b, since both  $\tau_a$  and  $\tau_i$  are now much longer than the age of the system.

In addition, the remnant eccentricity could be maintained due to weak damping of the tide in the star for the same reasons. However, we must also explain the inefficient damping of the tide in the planet, if indeed the reason for the eccentricity is that  $\tau_e > \tau_*$ . The planet in this system is massive, and may be a low-mass brown dwarf. If it formed without a core, then the dissipation of inertial modes may be reduced if they are able to form global modes, as found in OL04.

An alternative explanation for the survival of XO-3 b involving a larger initial semi-major axis for the planet is also possible, but this would require significant tidal migration to bring the planet to its current location. This would require a much lower stellar  $Q'$  than our calculations predict, which as discussed in §3.1 would imply a very short inspiral time for the planets on the tightest orbits, if their host stars have similar  $Q'$  values. We discuss this further with regards to the host stars WASP-12 and OGLE-TR-56 in §8.3 below.

## 8.2 Tidal dissipation in F-stars

Our calculation of  $Q'$  for XO-3, indicates that it would be worthwhile to study the range of  $Q'$  expected for F-stars, and how these may differ from solar-type stars. We performed calculations of tidal dissipation in the OCZs of a variety of F-stars between the masses of  $1.2 - 1.6 M_\odot$ , using the numerical method of OL07, and the stellar models of EZ-Evolution. These stars contain convective cores surrounded by a radiative zone and an OCZ, and for the reasons mentioned in the previous section, we expect that tidal dissipation in the OCZ will dominate the dissipation. We consider the range of OCZ properties in F-stars, as the mass and metallicity are varied. Below we present a selection of illustrative examples, which represent the range of properties expected for F-stars.

Fig. 8 shows  $Q'$  as a function of tidal frequency for two F-stars, with different OCZ properties. Fig. 8(a) shows that tidal dissipation in more massive F-stars, with very thin OCZs, is found to be extremely weak, with  $Q' \geq 10^{12}$  for most tidal frequencies. This implies that tidal dissipation in such stars is probably negligible in contributing to the spin-orbit evolution of HJs. Fig. 8(b) shows that tidal dissipation in lower mass F-stars with thicker convective envelopes, is similar to but slightly weaker than, that for solar-type stars (OL07), since  $Q' \sim 10^8$  for most tidal frequencies in the range  $|\hat{\omega}| < 2|\Omega|$ .

A model with  $1.3 M_\odot$  star similar to XO-3, except that we choose supersolar metallicity ( $Z = 0.03$ ), is found to have a similar OCZ to the  $1.2 M_\odot$  model in Fig. 8(b), and has a very similar  $Q'$ . The metallicity of the star affects the thickness of the OCZ, and therefore the efficiency of tidal dissipation.

From these examples, it is clear that assuming a single  $Q'$  applies for all stars is probably incorrect. Even within the mass range of F-stars there is considerable variation in  $Q' \sim 10^8 - 10^{12}$  in our calculations, primarily as a result of the variation in the mass fraction contained in the OCZ. There are also differences between G and F stars, due to differences in internal structure – most notably the presence of

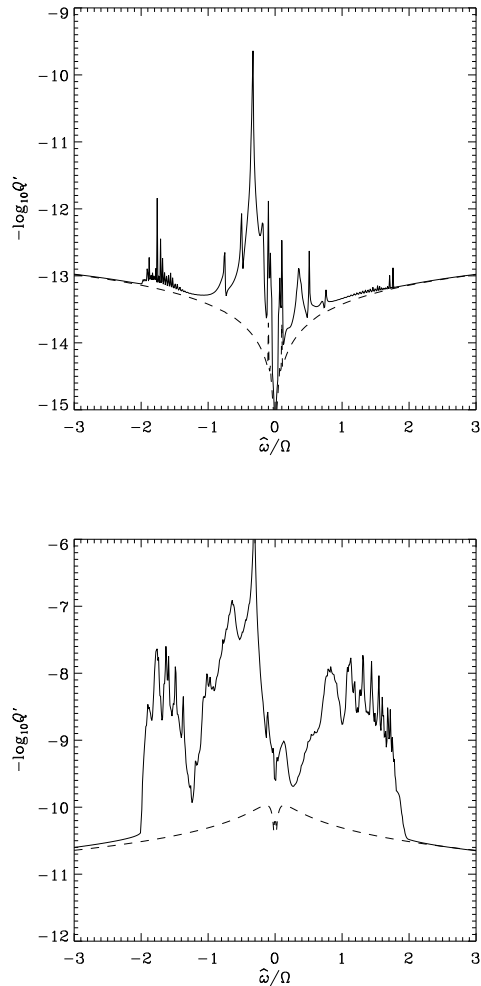


**Figure 8.** Tidal  $Q'$ -factor as a function of the ratio of tidal frequency to spin frequency  $\hat{\omega}/\Omega$ , from dissipation of the  $l = m = 2$  component (we find the behaviour of the  $m = 0$  and 1 components is similar in magnitude) of the equilibrium tide, and dissipation of inertial modes, in the OCZ of two F-type star models. The dashed lines represent the effect of omitting the Coriolis force, and therefore inhibiting inertial waves. The top figure shows a high-mass  $1.5 M_{\odot}$  F-star, with solar metallicity and an age of 0.7 Gyr, assumed to be spinning with a period of 3 d. This has a very thin OCZ, and tidal dissipation is extremely weak. The bottom figure shows a low-mass  $1.2 M_{\odot}$  F-star, with solar metallicity and an age of 1.0 Gyr, assumed to be spinning with a period of 3 d. Tidal dissipation is much stronger in this star, though still smaller than that in Fig. 6 from OL07 for a  $1.0 M_{\odot}$  G-star. Together with Fig. 7 this shows that  $Q'$  can vary considerably between different stars, even within the range of F-stars.

a radiative core in a G-type star may lead to enhanced dissipation by nonlinear effects. Lower mass stars, and those with higher metallicity, tend to have thicker OCZs than higher mass, low-metallicity stars. In addition, higher mass stars are more centrally condensed, so the mass fraction in their outer regions will be lower. This results in low-mass, high-metallicity stars having lower  $Q'$  than high-mass, low-metallicity stars. In addition, OLO7 found that the spin period of the star also affects  $Q'$ .

### 8.3 The survival of WASP-12 b and OGLE-TR-56 b

The results of the last two sections also allow us to propose an explanation for the survival of the planets on the tightest orbits, such as WASP-12 b (Hebb et al. 2008) and OGLE-TR-56 b (Sasselov 2003). Taking the current values for the stellar properties of the host stars in both systems, we find that they are both likely to have a similar internal structure to those discussed above, with a convective core present, which will prevent internal inertia-gravity waves from reaching the centre of each star. In addition, these stars are slowly rotating, and so the relevant tidal frequencies are likely to be outside the range of inertial waves ( $|\hat{\omega}| > 2|\Omega|$ ), which would imply that such waves are not excited by tidal forcing. This means that  $Q'$  is likely to be much larger than that in the models discussed above (in Fig. 8), particularly since reducing the spin frequency is found to increase  $Q'$  for a given ratio  $\hat{\omega}/\Omega$  (OL07). Therefore it is likely that the relevant  $Q' \gtrsim 10^{10}$ , which would imply that tidally induced inspiral will not occur within the age of the system. This means that weak dissipation in the star could potentially explain the survival of both of these planets.

## 9 CONCLUSIONS

In this paper we have investigated the long-term tidal evolution of close-in extrasolar planets. We studied the effects of magnetic braking on tidal evolution in a simplified system, and then performed numerical integrations for a variety of HJ systems, with particular emphasis on inclination evolution. We now summarise the main results of this work.

Magnetic braking moves the corotation radius of the star outwards such that any close-in planets will eventually orbit inside corotation ( $\Omega \cos i < n$ ), and be subject to orbital decay due to tides. It makes no sense to refer to any close-in planet as being *tidally evolved*, since magnetic braking removes the only equilibrium state accessible through tidal friction during the expected stellar lifetime.

Magnetic braking is found to be important for the tidal evolution of HJs unless  $\Omega \cos i \ll n$ , in which case the orbit is already well inside the orbit-projected corotation radius. Highly inclined (especially retrograde) orbits tend to be affected less by magnetic braking, since this condition is often satisfied regardless of the spin rate. Magnetic braking is particularly important when it comes to interpreting the tidal evolution of observed systems from formation to the present day, since the star may have been rotating much more rapidly in the past. Nevertheless, it is probably not a bad approximation to neglect magnetic braking for calculating the *future* tidal evolution of most observed HJs, if the star has already spun down so that  $\Omega \ll n$ .

Combining our results with those of Jackson et al. (2008a), we find that coupled evolution of the orbital and rotational elements is essential to accurately model tidal evolution, and can result in much faster evolution than simple timescale estimates predict. This is especially true for highly eccentric orbits, for which the associated semi-major axis evolution increases the rate of stellar spin-orbit alignment by up to several orders of magnitude.

We find that the true timescale for stellar spin-orbit

alignment is comparable to the inspiral time for HJs, therefore the orbits of most close-in planets have probably not aligned with the spin of the star. Observed inclinations are likely to be a relic of the migration process. This means that RM observations of transiting planets can potentially distinguish between migration caused by planet–planet scattering or Kozai oscillations combined with tidal dissipation in the star, and that produced by tidal interaction with the gas disc. If the majority of candidates are found with  $\lambda \sim 0$ , this strongly disfavours planet–planet scattering or Kozai migration, since they are expected to produce significantly inclined orbits, and we have found that tides are unlikely to have aligned orbits without causing inspiral. Alternatively, if systems are found with significantly nonzero  $\lambda$ , then some planet–planet scattering or Kozai migration could have occurred to produce these orbital inclinations. We strongly encourage future observations of the RM effect for transiting planets.

For most HJs, tides tends to circularise the planet’s orbit before spin–orbit alignment or inspiral occurs. If an orbit is initially inclined and eccentric, as a result of planet–planet scattering or Kozai migration into a short–period orbit, then we would expect the orbit to become circular before it aligns. Therefore, if we observe a planet on an inclined, circular orbit, we cannot rule out a non-negligible eccentricity in the past. This means that we should observe fewer eccentric orbits than inclined orbits *if those systems start with a uniform distribution of points in  $(e, i)$ -space*, due to tidal friction. This should be considered when comparing the observed  $(e, i)$  distribution with those predicted from theoretical work on Kozai migration or planet–planet scattering, before we can further constrain these theories (Fabrycky & Tremaine 2007; Jurić & Tremaine 2008).

The misaligned spin and orbit of the XO-3 system could potentially be explained in terms of inefficient tidal dissipation inside the host star. The required stellar  $Q'_1 \gtrsim 10^{10}$  required for the survival and remnant misalignment is predicted from theoretical calculations of tidal dissipation in the OCZ of an F–star. In addition, the remnant eccentricity poses constraints on the planetary  $Q'_2 \gtrsim 10^8$ , in the absence of perturbing forces that could excite the eccentricity.

The stellar  $Q'$  has been shown to vary widely between different stars, and even within the range of F–stars, from  $10^8 - 10^{12}$ . There are also differences between  $Q'$  for the F–star models discussed here, and the solar–type star models discussed in OL07. This implies that assuming a single value of  $Q'$  applies to all exoplanet host stars is probably incorrect.  $Q'$  has been found to vary with stellar mass, metallicity, spin period, as well as tidal frequency. The presence of a convective core is likely to be important, in that it acts to prevent internal inertia–gravity waves, which are excited at the interface between the convective and radiative zones, from reaching the centre of the star, where nonlinear effects could enhance their dissipation. This may explain the survival of some of the planets on the tightest orbits, such as WASP-12 b and OGLE-TR-56 b, whose host stars are likely to have convective cores.

It is clear that much more work is required to study the mechanisms of tidal dissipation in rotating stars. It would also be useful to perform a detailed study into the possibility of core–envelope decoupling in such stars, since this may have implications for the survival and remnant inclinations

of close-in planets. Future observations of transiting planets will constrain these theories, hopefully leading to a better understanding of the mechanisms at work in the formation and evolution of planetary systems.

## ACKNOWLEDGMENTS

We would like to thank the referee, Richard Greenberg, for helpful comments that have improved the manuscript. In addition, A.J.B would like to thank STFC for a research studentship.

## APPENDIX A: TIDAL EVOLUTION EQUATIONS

Here we present the orbit-averaged tidal evolution equations (Eggleton et al. 1998; Eggleton & Kiseleva-Eggleton 2001; Mardling & Lin 2002) used in this work. These are derived starting with the equation of relative motion of a planet of mass  $m_2$  and its host star of mass  $m_1$

$$\frac{d^2 \mathbf{r}}{dt^2} = -\frac{Gm_{12}}{r^3} \mathbf{r} + \mathbf{f}, \quad (\text{A1})$$

where  $\mathbf{r}$  is the separation,  $m_{12} = m_1 + m_2$ , and  $\mathbf{f}$  represents a perturbing acceleration. In Eggleton & Kiseleva-Eggleton (2001),  $\mathbf{f}$  contains many contributions: the effects of general relativity, perturbing accelerations due to other planets and tidal and spin distortions of the star and planet, as well as tidal friction. Here we solely consider the perturbing effects of tidal friction and set  $\mathbf{f} = \mathbf{f}_{\text{tf}} = \mathbf{f}_{\text{tf}}^1 + \mathbf{f}_{\text{tf}}^2$ , where

$$\mathbf{f}_{\text{tf}}^{1,2} = -3\tau_{1,2} k_{1,2} n^2 \left( \frac{m_{2,1}}{m_{1,2}} \right) \left( \frac{R_{1,2}}{a} \right)^5 \left( \frac{a}{r} \right)^8 [3(\hat{\mathbf{r}} \cdot \dot{\mathbf{r}}) \hat{\mathbf{r}} + (\hat{\mathbf{r}} \times \dot{\mathbf{r}} - r \boldsymbol{\Omega}_{1,2}) \times \hat{\mathbf{r}}]. \quad (\text{A2})$$

Here  $n = \sqrt{\frac{Gm_{12}}{a^3}}$  is the orbital mean motion,  $k_{1,2}$  are the second-order potential Love numbers for the star and planet respectively (which is twice the apsidal motion constant), and  $\tau_{1,2}$  is the effective tidal lag time for each body. This form of the dissipative force of tidal friction is that derived under the assumption of a constant lag time in the equilibrium tide model (Eggleton et al. 1998). In this model, we assume that the body quasi-hydrostatically adjusts to the perturbing potential of its companion, but delayed by some small lag time ( $\tau_1$  for the star,  $\tau_2$  for the planet) that is proportional to the dissipation. Thus for each body,  $Q = \frac{1}{\omega\tau}$  is assumed to be inversely proportional to the tidal frequency  $\hat{\omega}$ , so that the lag time  $\tau$  is independent of tidal frequency, and is therefore the same for all components of the tide. This model is beneficial because the resulting secular evolution equations can treat arbitrary orbital eccentricities and stellar and planetary obliquities.

In the resulting equations we have chosen to parametrise the efficiency of tidal dissipation in each body by redefining  $Q = \frac{1}{n\tau}$ , and adopt a constant  $Q$  which does not change during the evolution i.e. we assume effectively that the lag time scales with the orbital period (then Eq. A2 matches Eq. 4 in Mardling & Lin 2002, where this assumption was not made explicit). We also introduce the definition  $Q' = \frac{3Q}{2k}$ , as discussed in §3.1. This allows us to discuss “ $Q'$  values” for particular bodies, which do not change as the orbital and rotational elements vary. For the purposes of this paper we *define*  $Q' = \frac{3}{2kn\tau}$ . This is equivalent to *assuming* that the relevant tidal frequency  $\hat{\omega} = n$ . Note that this may not give identical numerical factors in the resulting equations to other formulations of tidal friction (e.g. Goldreich & Soter 1966; Zahn 1977; Hut 1981), but we feel that this is the best way to study the general effects of tidal friction, given our uncertainties in the value of  $Q'$ , and its dependence on  $\hat{\omega}$ , for realistic giant planets and stars.

The secular evolution of the orbital elements is calculated via the specific orbital angular momentum vector  $\mathbf{h} = \mathbf{r} \times \dot{\mathbf{r}} = na^2 \sqrt{1-e^2} \hat{\mathbf{h}}$ , and the eccentricity vector  $\mathbf{e}$ . The eccentricity vector has the magnitude of the eccentricity, and points in the direction of periastron, and is given by

$$\mathbf{e} = \frac{\dot{\mathbf{r}} \times \mathbf{h}}{Gm_{12}} - \hat{\mathbf{r}}. \quad (\text{A3})$$

The planet’s specific orbital angular momentum  $\mathbf{h}$  changes at a rate

$$\frac{d\mathbf{h}}{dt} = \mathbf{r} \times (\mathbf{f}_{\text{tf}}^1 + \mathbf{f}_{\text{tf}}^2), \quad (\text{A4})$$

with a corresponding rate of angular momentum transfer between the orbit and spin of each body given by

$$\dot{\mathbf{J}}_{1,2} = I_{1,2} \dot{\boldsymbol{\Omega}}_{1,2} = -\mu \mathbf{r} \times \mathbf{f}_{\text{tf}}^{1,2}, \quad (\text{A5})$$

since total angular momentum is conserved, and where  $\mu = \frac{m_1 m_2}{m_{12}}$  is the reduced mass of the system. The eccentricity vector evolves as

$$\frac{d\mathbf{e}}{dt} = \frac{[2(\mathbf{f}_{\text{tf}} \cdot \dot{\mathbf{r}}) \mathbf{r} - (\mathbf{r} \cdot \dot{\mathbf{r}}) \mathbf{f}_{\text{tf}} - (\mathbf{f}_{\text{tf}} \cdot \mathbf{r}) \dot{\mathbf{r}}]}{Gm_{12}}. \quad (\text{A6})$$

Eqs. A4 and A6 are time-averaged over the orbit of the planet, and the resulting differential equations are given below. Numerical integration of these equations gives the secular evolution of the orbital elements. Note that we have written these equations so that they are regular at  $e = 0$ , unlike those in Eggleton & Kiseleva-Eggleton (2001) and Mardling & Lin (2002) – we eliminate reference to the basis vectors chosen in their representation, since  $\hat{\mathbf{e}}$  is undefined for a circular orbit, whereas  $\mathbf{e}$  is well defined and equal to zero.



$$\frac{d\mathbf{h}}{dt} = -\frac{1}{t_{f1}} \left[ \frac{\boldsymbol{\Omega}_1 \cdot \mathbf{e}}{2n} f_5(e^2) h \mathbf{e} - \frac{\boldsymbol{\Omega}_1}{2n} f_3(e^2) h + \left( f_4(e^2) - \frac{\boldsymbol{\Omega}_1 \cdot \mathbf{h}}{2n} \frac{1}{h} f_2(e^2) \right) \mathbf{h} \right] \quad (\text{A7})$$

$$-\frac{1}{t_{f2}} \left[ \frac{\boldsymbol{\Omega}_2 \cdot \mathbf{e}}{2n} f_5(e^2) h \mathbf{e} - \frac{\boldsymbol{\Omega}_2}{2n} f_3(e^2) h + \left( f_4(e^2) - \frac{\boldsymbol{\Omega}_2 \cdot \mathbf{h}}{2n} \frac{1}{h} f_2(e^2) \right) \mathbf{h} \right] \quad (\text{A8})$$

$$= \left( \frac{d\mathbf{h}}{dt} \right)_1 + \left( \frac{d\mathbf{h}}{dt} \right)_2 \quad (\text{A9})$$

$$h \frac{d\mathbf{e}}{dt} = -\frac{1}{t_{f1}} \left[ \frac{\boldsymbol{\Omega}_1 \cdot \mathbf{e}}{2n} f_2(e^2) \mathbf{h} + 9 \left( f_1(e^2) h - \frac{11}{18} \frac{\boldsymbol{\Omega}_1 \cdot \mathbf{h}}{n} f_2(e^2) \right) \mathbf{e} \right] \quad (\text{A10})$$

$$-\frac{1}{t_{f2}} \left[ \frac{\boldsymbol{\Omega}_2 \cdot \mathbf{e}}{2n} f_2(e^2) \mathbf{h} + 9 \left( f_1(e^2) h - \frac{11}{18} \frac{\boldsymbol{\Omega}_2 \cdot \mathbf{h}}{n} f_2(e^2) \right) \mathbf{e} \right] \quad (\text{A11})$$

$$\frac{d\boldsymbol{\Omega}_1}{dt} = -\frac{\mu}{I_1} \left( \frac{d\mathbf{h}}{dt} \right)_1 + \dot{\boldsymbol{\omega}}_{\text{mb}} \quad (\text{A12})$$

$$= \frac{\mu}{I_1 t_{f1}} \left[ \frac{\boldsymbol{\Omega}_1 \cdot \mathbf{e}}{2n} f_5(e^2) h \mathbf{e} - \frac{\boldsymbol{\Omega}_1}{2n} f_3(e^2) h + \left( f_4(e^2) - \frac{\boldsymbol{\Omega}_1 \cdot \mathbf{h}}{2n} \frac{1}{h} f_2(e^2) \right) \mathbf{h} \right] + \dot{\boldsymbol{\omega}}_{\text{mb}} \quad (\text{A13})$$

$$\frac{d\boldsymbol{\Omega}_2}{dt} = -\frac{\mu}{I_2} \left( \frac{d\mathbf{h}}{dt} \right)_2 \quad (\text{A14})$$

$$= \frac{\mu}{I_2 t_{f2}} \left[ \frac{\boldsymbol{\Omega}_2 \cdot \mathbf{e}}{2n} f_5(e^2) h \mathbf{e} - \frac{\boldsymbol{\Omega}_2}{2n} f_3(e^2) h + \left( f_4(e^2) - \frac{\boldsymbol{\Omega}_2 \cdot \mathbf{h}}{2n} \frac{1}{h} f_2(e^2) \right) \mathbf{h} \right] \quad (\text{A15})$$

We also need to define an inverse tidal friction timescale  $t_f^{-1}$  for each body (here for body 1, change  $1 \rightarrow 2$  to get the corresponding expression for body 2), and the functions of the eccentricity (first derived in a similar form by Hut 1981).

$$\frac{1}{t_{f1}} = \left( \frac{9n}{2Q'_1} \right) \left( \frac{m_2}{m_1} \right) \left( \frac{R_1}{a} \right)^5 = \sqrt{Gm_{12}} \left( \frac{9}{2Q'_1} \right) \left( \frac{m_2}{m_1} \right) R_1^5 a^{-\frac{13}{2}} \quad (\text{A16})$$

$$f_1(e^2) = \frac{1 + \frac{15}{4}e^2 + \frac{15}{8}e^4 + \frac{5}{64}e^6}{(1 - e^2)^{\frac{13}{2}}} \quad (\text{A17})$$

$$f_2(e^2) = \frac{1 + \frac{3}{2}e^2 + \frac{1}{8}e^4}{(1 - e^2)^5} \quad (\text{A18})$$

$$f_3(e^2) = \frac{1 + \frac{9}{2}e^2 + \frac{5}{8}e^4}{(1 - e^2)^5} \quad (\text{A19})$$

$$f_4(e^2) = \frac{1 + \frac{15}{2}e^2 + \frac{45}{8}e^4 + \frac{5}{16}e^6}{(1 - e^2)^{\frac{13}{2}}} \quad (\text{A20})$$

$$f_5(e^2) = \frac{3 + \frac{1}{2}e^2}{(1 - e^2)^5} \quad (\text{A21})$$

$$f_6(e^2) = \frac{1 + \frac{31}{2}e^2 + \frac{255}{8}e^4 + \frac{185}{16}e^6 + \frac{25}{64}e^8}{(1 - e^2)^8} \quad (\text{A22})$$

$$(\text{A23})$$

In the absence of magnetic braking ( $\dot{\boldsymbol{\omega}}_{\text{mb}} = \mathbf{0}$ ) the total angular momentum is conserved ( $\frac{d\mathbf{L}}{dt} = \mathbf{0}$ ). With the inclusion of magnetic braking, the total angular momentum of the system decreases at a rate

$$\frac{d\mathbf{L}}{dt} = \frac{d}{dt} (\mu \mathbf{h} + I_1 \boldsymbol{\Omega}_1 + I_2 \boldsymbol{\Omega}_2) = I_1 \dot{\boldsymbol{\omega}}_{\text{mb}} = -\alpha_{\text{mb}} I_1 \Omega_1^2 \boldsymbol{\Omega}_1. \quad (\text{A24})$$

Tidal dissipation and magnetic braking result in a loss of energy from the system. The total rate of energy dissipated can be expressed as follows:

$$\dot{E}_{\text{tot}} = \frac{1}{2} \frac{Gm_1 m_2}{a} \frac{\dot{a}}{a} + I_1 \Omega_1 \dot{\Omega}_1 + I_2 \Omega_2 \dot{\Omega}_2 \quad (\text{A25})$$

$$= H_1 + H_2 - \alpha_{\text{mb}} I_1 \Omega_1^4, \quad (\text{A26})$$

where the final term in the last expression is the energy dissipated by magnetic braking and

$$H_1 = -\frac{\mu h}{n t_{f1}} \left[ \frac{1}{2} \left( \Omega_1^2 f_3(e^2) + \frac{(\boldsymbol{\Omega}_1 \cdot \mathbf{h})^2}{h^2} f_2(e^2) - (\boldsymbol{\Omega}_1 \cdot \mathbf{e})^2 f_5(e^2) \right) - 2n \frac{(\boldsymbol{\Omega}_1 \cdot \mathbf{h})}{h} f_4(e^2) + n^2 f_6(e^2) \right], \quad (\text{A27})$$

$$H_2 = -\frac{\mu h}{n t_{f2}} \left[ \frac{1}{2} \left( \Omega_2^2 f_3(e^2) + \frac{(\boldsymbol{\Omega}_2 \cdot \mathbf{h})^2}{h^2} f_2(e^2) - (\boldsymbol{\Omega}_2 \cdot \mathbf{e})^2 f_5(e^2) \right) - 2n \frac{(\boldsymbol{\Omega}_2 \cdot \mathbf{h})}{h} f_4(e^2) + n^2 f_6(e^2) \right], \quad (\text{A28})$$

are the tidal heating rates in the star and planet, respectively. It has been proposed that  $H_2$  can result in planetary inflation,

if the energy is deposited deep in the interior of the planet (Bodenheimer et al. 2001; Jackson et al. 2008b). Note that these expressions approach zero as  $e \rightarrow 0$ ,  $\boldsymbol{\Omega}_{1,2} \cdot \mathbf{e} \rightarrow 0$  and  $\boldsymbol{\Omega}_{1,2} \cdot \mathbf{h} \rightarrow n$  i.e. tidal dissipation continues until the orbit becomes circular, and the spin of each body becomes coplanar and synchronous with the orbit.

## APPENDIX B: TIDAL POTENTIAL EXPANDED TO ARBITRARY ORDER IN STELLAR OBLIQUITY

In this section we expand the tidal potential into its separate Fourier components, following the approach of OL04. We aim to study which tidal frequencies are relevant for highly inclined orbits, such as that of XO-3 b. We consider two bodies in mutual Keplerian orbit with semi-major axis  $a$  and mean motion  $n$ . Adopt a coordinate system with origin at the centre of body 1, and let this represent the star, and body 2 the planet. The tidal potential experienced at an arbitrary point P in body 1 is the nontrivial term of lowest order in  $r$ ,

$$\Psi = \frac{Gm_2}{2R^5} [R^2 r^2 - 3(\mathbf{R} \cdot \mathbf{r})^2], \quad (\text{B1})$$

where position vector of the point P in body 1 is  $\mathbf{r}$ , and the position vector of the centre of mass of body 2 is  $\mathbf{R}(t)$ . Body 2 is treated as a point mass, of mass  $m_2$ . We consider an inclined, circular orbit. Without loss of generality, we consider body 2 to orbit in a plane inclined to the  $(x, y)$ -plane by an angle  $i$ , so that its Cartesian coordinates are

$$\mathbf{R} = a (\cos nt \cos i, \sin nt, \cos nt \sin i), \quad (\text{B2})$$

while the Cartesian coordinates of a point P are

$$\mathbf{r} = r (\sin \theta \cos \phi, \sin \theta \sin \phi, \cos \theta), \quad (\text{B3})$$

where  $(r, \theta, \phi)$  are the usual spherical polar coordinates. Then

$$\Psi = \frac{Gm_2}{2a^3} r^2 [1 - 3(\cos nt \cos i \sin \theta \cos \phi + \sin nt \sin \theta \sin \phi + \cos nt \sin i \cos \theta)^2]. \quad (\text{B4})$$

Let

$$\tilde{P}_l^m(\cos \theta) = \left[ \frac{(2l+1)(l-m)!}{2(l+m)!} \right]^{\frac{1}{2}} P_l^m(\cos \theta), \quad (\text{B5})$$

where  $0 \leq m \leq l$  and  $l \in \mathbb{Z}^+$ , denote an associated Legendre polynomial normalised such that

$$\int_0^\pi [\tilde{P}_l^m(\cos \theta)]^2 \sin \theta d\theta = 1. \quad (\text{B6})$$

The tidal potential correct to arbitrary order in the stellar obliquity  $i$  can be expanded as a series of rigidly rotating solid spherical harmonics of second degree,

$$\Psi = \frac{Gm_2}{a^3} \left[ \sum_{j=1}^8 A_j(i) r^2 \tilde{P}_2^{m_j}(\cos \theta) \cos(m_j \phi - \omega_j t) \right], \quad (\text{B7})$$

where the azimuthal order  $m_j$ , frequency  $\omega_j$ , tidal (Doppler-shifted) forcing frequency  $\hat{\omega}_j = \omega_j - m_j \Omega$ , and the obliquity dependent amplitude  $A_j(i)$  of each component are

$$m_1 = 0, \quad \omega_1 = 0, \quad \hat{\omega}_1 = 0, \quad A_1 = \sqrt{\frac{1}{10}} \left( 1 - \frac{3}{2} \sin^2 i \right), \quad (\text{B8})$$

$$m_2 = 2, \quad \omega_2 = 2n, \quad \hat{\omega}_2 = 2n - 2\Omega, \quad A_2 = -\sqrt{\frac{3}{5}} \cos^4 \frac{i}{2}, \quad (\text{B9})$$

$$m_3 = 0, \quad \omega_3 = 2n, \quad \hat{\omega}_3 = 2n, \quad A_3 = -\frac{3}{2} \sqrt{\frac{1}{10}} \sin^2 i, \quad (\text{B10})$$

$$m_4 = 1, \quad \omega_4 = 0, \quad \hat{\omega}_4 = -\Omega, \quad A_4 = \sqrt{\frac{3}{5}} \cos i \sin i, \quad (\text{B11})$$

$$m_5 = 1, \quad \omega_5 = 2n, \quad \hat{\omega}_5 = 2n - \Omega, \quad A_5 = \frac{1}{2} \sqrt{\frac{3}{5}} \sin i (\cos i + 1), \quad (\text{B12})$$

$$m_6 = 1, \quad \omega_6 = -2n, \quad \hat{\omega}_6 = -2n - \Omega, \quad A_6 = \frac{1}{2} \sqrt{\frac{3}{5}} \sin i (\cos i - 1), \quad (\text{B13})$$

$$m_7 = 2, \quad \omega_7 = 0, \quad \hat{\omega}_7 = -2\Omega, \quad A_7 = \frac{1}{2} \sqrt{\frac{3}{5}} \sin^2 i, \quad (\text{B14})$$

$$m_8 = 2, \quad \omega_8 = -2n, \quad \hat{\omega}_8 = -2n - 2\Omega, \quad A_8 = -\sqrt{\frac{3}{5}} \sin^4 \frac{i}{2}. \quad (\text{B15})$$

There are eight components of the tide that contribute for arbitrary stellar obliquity. For small inclination, the terms that are of first order in the obliquity are for  $m = 1$  and are the  $j = 4$  and  $j = 5$  components above (not the component having tidal frequency  $\hat{\omega} = n - \Omega$ , as incorrectly stated in OL04). For a coplanar orbit, only  $j = 1$  and  $j = 2$  components above contribute, and these reduce to the first two components in OL04.

For an orbit at  $i \sim 90^\circ$ , all components except  $j = 2$  and  $j = 4$  contribute to the tidal force. Thus, for XO-3, it is important to calculate the resulting  $Q'$  for the  $m = 0$ ,  $m = 1$  and  $m = 2$  components of the tide. The relevant tidal frequencies for this system cannot be calculated with any certainty, since the stellar spin period has not been accurately determined. If we assume that the angle of inclination of the stellar equatorial plane to the plane of the sky is  $\sim 90^\circ$ , then we have  $\Omega \sim n$  currently. The relevant tidal frequencies would then be  $\hat{\omega} = 0, \pm\Omega, \pm 2\Omega, \pm 3\Omega, \pm 4\Omega$ .

## REFERENCES

- Barnes R., Greenberg R., 2007, *ApJL*, 665, L67
- Barnes S. A., 2003, *ApJ*, 586, 464
- Bodenheimer P., Lin D. N. C., Mardling R. A., 2001, *ApJ*, 548, 466
- Chatterjee S., Ford E. B., Matsumura S., Rasio F. A., 2008, *ApJ*, 686, 580
- Cochran W. D., Redfield S., Endl M., Cochran A. L., 2008, *ApJL*, 683, L59
- Counselman III C. C., 1973, *ApJ*, 180, 307
- Cresswell P., Dirksen G., Kley W., Nelson R. P., 2007, *A&A*, 473, 329
- Dobbs-Dixon I., Lin D. N. C., Mardling R. A., 2004, *ApJ*, 610, 464
- Donati J.-F., Moutou C., Farès R., Bohlender D., Catala C., Deleuil M., Shkolnik E., Cameron A. C., Jardine M. M., Walker G. A. H., 2008, *MNRAS*, 385, 1179
- Eggleton P. P., Kiseleva L. G., Hut P., 1998, *ApJ*, 499, 853
- Eggleton P. P., Kiseleva-Eggleton L., 2001, *ApJ*, 562, 1012
- Fabrycky D., Tremaine S., 2007, *ApJ*, 669, 1298
- Ford E. B., Rasio F. A., 2008, *ApJ*, 686, 621
- Goldreich P., Soter S., 1966, *Icarus*, 5, 375
- Goodman J., Dickson E. S., 1998, *ApJ*, 507, 938
- Greenberg R., 1974, *Icarus*, 23, 51
- Hebb L., Collier-Cameron A., Loeillet B., Pollacco D., Super-Wasp Consortium t., 2008, *ArXiv e-prints*
- Hébrard G., Bouchy F., Pont F., et al., 2008, *A&A*, 488, 763
- Holzwarth V., Jardine M., 2005, *A&A*, 444, 661
- Hut P., 1980, *A&A*, 92, 167
- Hut P., 1981, *A&A*, 99, 126
- Ivanova N., Taam R. E., 2003, *ApJ*, 599, 516
- Jackson B., Greenberg R., Barnes R., 2008a, *ApJ*, 678, 1396
- Jackson B., Greenberg R., Barnes R., 2008b, *ApJ*, 681, 1631
- Johns-Krull C. M., McCullough P. R., Burke C. J., Valenti J. A., Janes K. A., Heasley J. N., Prato L., Bissinger R., Fleener M., Foote C. N., Garcia-Melendo E., Gary B. L., Howell P. J., Mallia F., Masi G., Vanmunster T., 2008, *ApJ*, 677, 657
- Jurić M., Tremaine S., 2008, *ApJ*, 686, 603
- Lin D. N. C., Bodenheimer P., Richardson D. C., 1996, *Nature*, 380, 606
- Lubow S. H., Ogilvie G. I., 2001, *ApJ*, 560, 997
- MacGregor K. B., Brenner M., 1991, *ApJ*, 376, 204
- Marcy G. W., Butler R. P., Williams E., Bildsten L., Graham J. R., Ghez A. M., Jernigan J. G., 1997, *ApJ*, 481, 926
- Mardling R. A., Lin D. N. C., 2002, *ApJ*, 573, 829
- Mayor M., Queloz D., 1995, *Nature*, 378, 355
- McLaughlin D. B., 1924, *ApJ*, 60, 22
- Murray C. D., Dermott S. F., 1999, *Solar system dynamics. Solar system dynamics by Murray, C. D., 1999*
- Nagasawa M., Ida S., Bessho T., 2008, *ApJ*, 678, 498
- Narita N., Sato B., Ohshima O., Winn J. N., 2008, *PASJ*, 60, L1+
- Ogilvie G. I., Lin D. N. C., 2004, *ApJ*, 610, 477
- Ogilvie G. I., Lin D. N. C., 2007, *ApJ*, 661, 1180
- Papaloizou J. C. B., Nelson R. P., Kley W., Masset F. S., Arty-mowicz P., 2007, in Reipurth B., Jewitt D., Keil K., eds, *Protostars and Planets V Disk-Planet Interactions During Planet Formation*. pp 655–668
- Papaloizou J. C. B., Savonije G. J., 1997, *MNRAS*, 291, 651
- Papaloizou J. C. B., Terquem C., 2006, *Reports of Progress in Physics*, 69, 119
- Peale S. J., Lee M. H., 2002, *Science*, 298, 593
- Pont F., 2008, *ArXiv e-prints*
- Press W. H., Teukolsky S. A., Vetterling W. T., Flannery B. P., 1992, *Numerical recipes in FORTRAN. The art of scientific computing*. Cambridge: University Press, —c1992, 2nd ed.
- Rossiter R. A., 1924, *ApJ*, 60, 15
- Sasselov D. D., 2003, *ApJ*, 596, 1327
- Savonije G. J., Papaloizou J. C. B., 1997, *MNRAS*, 291, 633
- Savonije G. J., Papaloizou J. C. B., Albers F., 1995, *MNRAS*, 277, 471
- Skumanich A., 1972, *ApJ*, 171, 565
- Taam R. E., Spruit H. C., 1989, *ApJ*, 345, 972
- Verbunt F., Zwaan C., 1981, *A&A*, 100, L7
- Weber E. J., Davis L. J., 1967, *ApJ*, 148, 217
- Winn J. N., 2008, *ArXiv e-prints*, 807
- Winn J. N., Johnson J. A., Fabrycky D., Howard A. W., Marcy G. W., Narita N., Crossfield I. J., Suto Y., Turner E. L., Esquerdo G., Holman M. J., 2009, *ArXiv e-prints*
- Winn J. N., Noyes R. W., Holman M. J., Charbonneau D., Ohta Y., Taruya A., Suto Y., Narita N., Turner E. L., Johnson J. A., Marcy G. W., Butler R. P., Vogt S. S., 2005, *ApJ*, 631, 1215
- Witte M. G., Savonije G. J., 2002, *A&A*, 386, 222
- Wu Y., Murray N., 2003, *ApJ*, 589, 605
- Yoder C. F., Peale S. J., 1981, *Icarus*, 47, 1
- Zahn J.-P., 1977, *A&A*, 57, 383
- Zahn J.-P., 2008, in *EAS Publications Series Vol. 29 of EAS Publications Series, Tidal dissipation in binary systems*. pp 67–90